12-2015

Characterization of a Multi-Laminate Angle-Ply AF Patch for Annulus Fibrosus Repair

Ryan Borem
Clemson University, rborem@g.clemson.edu

CHARACTERIZATION OF A MULTI-LAMINATE ANGLE-PLY AF PATCH FOR ANNULUS FIBROSUS REPAIR

A Thesis
Presented to
the Graduate School of
Clemson University

In Partial Fulfillment
of the Requirements for the Degree
Master of Engineering
Bioengineering

---

by
Ryan Andrew Borem
December 2015

Accepted by:
Dr. Jeremy Mercuri, Committee Chair
Dr. Dan Simionescu
Dr. Sanjitpal Gill

ABSTRACT

Annually, over 5.7 million Americans are diagnosed with two IVD-associated pathologies: IVD herniation (IVDH- a mechanical disruption of the concentric fibrous layers of the annulus fibrosus (*AF*))) and degeneration (IVDD- a multifactorial process which initiates within the inner gelatinous core *(NP*), and results in a biochemical degradation of NP tissue), with over 2.7 million requiring surgical inteventions.[1,2] Although both underlying pathologies are different, quite often they both lead to a decrease in IVD height, impaired mechanical function, and increased pain and disability. These pain symptoms affect approximately 80% of the adult population during their lifetime with estimated expenditures exceeding $85.9 billion.[3,4]

Current surgical procedures for IVDH and IVDD are palliative and suffer from drawbacks. While they are performed to address patient symptoms, they fail to address the underlying pathology of a defect remaining within the subsequent layers of the AF. An effective AF closure/repair device in conjunction with a less aggressive discectomy for IVDH and/or NP arthroplasty for IVDD, may result in improved patient outcomes, decreased pain, and provide fewer revision surgeries via lower re-herniation and expulsion rates.[5,6] Therefore, an intact AF must be re-established to prevent implant expulsion or re-herniation, thus addressing the two major spinal pathologies directly associated with an IVD.

Currently within the medical device market, no tissue engineering biomaterials are available for AF closure/repair. Current market AF closure devices (Intrinsic Barricaid®, Anulex X-Close® Tissue Repair System, and Anulex Inclose® Surgical Mesh System) are

synthetic materials focused solely on preserving and reinforcing the native tissue and lack efficient strategies for implantation, fixation, and regeneration. Therefore, there has been an increase in tissue engineering and regenerative therapeutic approaches aiming for structural and biological AF repair investigated over the last decade using *in vivo* and *in vitro* experimentation. It is proposed that the optimum AF tissue engineering scaffold should reproduce the architecture, and the mechanical properties of the native human AF tissue.[7] Recent articles illustrate several novel suture, seal, and barrier techniques currently under development, resulting in an increasing attention at scientific workshops and conferences.[8–15]

To develop a tissue engineering biomaterial that is suitable for AF closure it must meet the following criteria: (1) mimic the structural angle-ply architecture of the native AF, (2) withstand static and dynamic mechanical properties mimicking the native functional characteristics, and (3) express cytocompatibility while promoting tissue regeneration. Current biomaterials growing attention in the tissue engineering academic field, electrospinning, polymers, glue, silk scaffolds, and honeycomb-scaffolds, require complex manufacturing procedures and typically work to address two of the three criteria (mimicking the biological and structural characteristics).[5] Although the mechanical advantage of closing annular defects to retain NP material seems intuitive, only recently have AF closure devices begun to examined in human cadaveric or animal tissues for their ability to withstand in situ IDP or flexibility testing.[16] Therefore, the use of decellularized tissue from a xenogeneic source is ideal due to its advantage of maintaining native extracellular matrix (ECM) while also removing all potential harmful xenogeneic factors.

We propose to address all three criteria with the development of a biomimetic angle-ply annulus fibrosus patch comprised of decellularized porcine pericardium. Porcine pericardium was chosen due to its native type I collagen content, mechanical strength, and cytocompatibility. The objectives of this research were to investigate the development of a biomimetic patch, consisting of decellularized porcine pericardium, to biologically augment AF repair by (1) characterizing the micro-architecture of the multi-laminate angle-ply AF patch, (2) evaluating the mechanical properties through static and dynamic tensile loading and impact resistance of IDP, and (3) evaluating the cytocompatibility of the patch using a healthy alternative cell source for AF tissue regeneration.

DEDICATION

This work is dedicated to the love of my life and to my mother. I would like to express my sincerest gratitude for their love and continued support throughout the years. Thank you Rose and Colleen for all the encouragement and assistance you have provided to me along the way. I greatly appreciate everything you have done.

ACKNOWLEDGMENTS

First, I would like to thank my mentor, Dr. Jeremy Mercuri, for his trust in my capabilities to conduct research within our laboratory (The Laboratory of Orthopaedic Tissue Regeneration and Orthobiologics). His kind works, guidance, support, and constant encouragement proved to be a great motivator and large influence in my work.

I would also like to thank all of my committee members; Dr. Sanjitipal Gill and Dr. Dan Simionescu for their insight, constructive criticisms, and advice in support of my research.

I would also like to thank all of my family, friends, and loves ones for their support throughout the years and for their constant guidance, unconditional love, and support. Especially my Aunt Mary and my brother Kevin.

I would also like to thank all of my fellow researchers in the OrthO-X lab. Their collaborations, teachings and time spent helping me with my work made this project conceivable. Additionally their comradery also helped make this experience exciting and memorable. I want to wish you all the best of luck in your future endeavors.

I would also like to thank my fellow classmates and professors here in the Bioengineering department of Clemson. There is no other department I would rather be a part of due to the support and respect between the students and professors.

Lastly, a special mention goes to my late cousin Mikie Eagen, greatly missed, who always believed in me and pushed me to be where I am today.

TABLE OF CONTENTS

Page

Table of Contents (Continued)

Page

Table of Contents (Continued)

Page

LIST OF TABLES

LIST OF FIGURES

CHAPTER I

LITERATURE REVIEW

BACKGROUND

Low back pain (LBP) affects approximately 80% of the adult population during their lifetime with estimated expenditures exceeding $85.9 billion.[3,4] Patients suffering from LBP often experience a diminished quality of life. Within the United States of America, LBP is the most common cause of activity limitation in people under the age of 45, the 2nd most frequent reason for doctor visits, the 5th leading cause of hospital admission, the 3rd most common surgical procedure, and the most common cause of job-related disability leading to days missed on the job.[2,17–19] Although LBP is multifactorial; LBP can originate from intervertebral disc (IVD) pathologies. Annually, over 5.7 million Americans are diagnosed with two IVD-associated pathologies: IVD herniation (IVDH- a mechanical disruption of the concentric fibrous layers of the annulus fibrosus (*AF*))) and degeneration (IVDD- a multifactorial process which initiates within the inner gelatinous core *(NP*), and results in a biochemical degradation of NP tissue), with over 2.7 million requiring surgical intervention.[1,2] Although both underlying pathologies are different, quite often they both lead to a decrease in IVD height, impaired mechanical function, and increased pain and disability.

INTERVERTEBRAL DISC ANATOMY, PHYSIOLOGY, AND PATHOLOGY

An IVD links adjacent vertebral bodies together to provide mobility and stability to the spine. The IVD's function is to support compressive loads arising from body weight and muscle forces while allowing for motion. There are 23 IVD's in the human spine: 6

cervical, 12 thoracic, 5 lumbar. The IVD is divided into three distinct regions as seen in **Figure 1**: nucleus pulposus (NP), annulus fibrosus (AF), and hyaline cartilaginous endplates.[20]

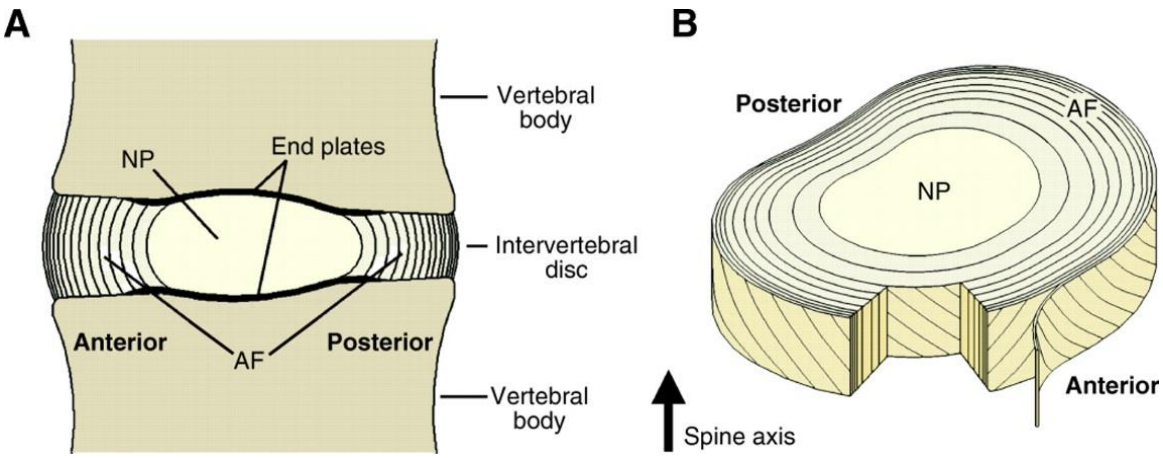

Figure 1: Intervertebral Disc Overview[21]

During early development, IVD's have some vascular supply to the cartilage endplates and AF, but these supplies quickly deteriorate leaving nearly no direct blood supply in healthy adults.[22] Thus, making these the largest, avascular structures in the human body. IVD's are composed of three major constituents: water, fibrillar collagens, and aggrecan (cartilage-specific proteoglycan). The proportion and organization of these components vary considerably with position across the IVD, for example, the NP has a higher concentration of aggrecan and water, but a lower collagen content than other regions of the IVD.[23] Collagen proportions change based on location in the IVD, with the NP containing only type II collagen while both types I and type II are found in the AF.[24]

The NP is the central proteoglycan and collagen Type II rich core distributes intradiscal pressure arising from applied compressive loads. The NP is comprised of a large aggregating proteoglycans, which contains a protein core. Up to 100 highly sulphated

glycosaminoglycan (GAG) chains, principally chondroitin and keratin sulphate, are covalently attached to a core protein.[25] The chains are long, linear carbohydrate polymers that have a net negative charge under physiological conditions. This negative charge attracts positively charged sodium ions which in return lures water molecules via osmosis. Research studies have proven a negative correlation between age and degeneration to the amount of water and GAGs present within the NP.[26] As GAGs begin to diminish overtime, it is replaced with fibrocartilage. The presence of fibrocartilage found in IVDs as GAGs diminish is a protective adaptation to physiological conditions.

The AF consists of circumferential exterior collagen sheets and is an essential constituent of the intervertebral joint. The AF is comprised of approximately 15-25 collagen sheets (lamellae), per IVD, which encompasses the NP.[27] These lamellae are comprised of type I collagen fibers that are aligned in alternating patterns of $\pm$ 30 degrees to the horizontal axis of the spine.[28] The AF can is divided into three layers: peripheral, intermediate, and inner regions. The annulus fibers are found to be thicker and more numerous anteriorly than posteriorly while the posterior fibers express a more parallel alignment.[29] The bundles of fibrous cartilage (multi-layers) runs obliquely from one vertebral body to the next to anchor the IVD to the cartilaginous endplates.

The hyaline cartilaginous endplates allow for nutrient supply to the IVD. Since IVD's are avascular structures, they are dependent on the endplates for nutrient diffusion. By the age of eight, the cartilaginous endplates lose their blood supply, leaving holes from blood vessels that allow for the diffusion of metabolites.[29] These holes which are essential

for the supply of nutrients also cause structural deficiencies (weakness) to the endplate structure.

CLINICAL SIGNIFICANCE OF INTERVERTEBRAL DISC DISEASES

In a clinical setting, two relevant pathologies directly affect the IVD: IVD herniation (IVDH) and IVD degeneration (IVDD). An IVDH is referred to as a "herniated disc", "bulging disc", or "slipped disc". IVDH as a consequence of traumatic (quick jolting motion), typically results in painful circumstances for the patient via nerve root impingement. As an IVDH begins to form, the AF begins to degrade and rupture progress radially through its layers. This results in a loss of IVD height, a decrease in IDP, and in many cases contributes significantly to LBP. This defect provides a pathway for the NP to bulge or migrate beyond the confines of the AF layers that can apply pressure to a nearby nerve within the spinal canal, "pinched nerve." The applied pressure leads to irritation of the nerve which depending on the level of intensity may lead to a radicular pair. Radicular pain is a pain that radiates to the extremities of the body, i.e. arm and legs, which travels directly along the course of a spinal nerve root. A "pinched nerve" may lead to symptoms of dull/sharp pain in the lower back, muscle spasms/cramping, sciatica, leg weakness, and/or loss of leg function. Although it is important to express, not all patients who develop an IVD herniation experience symptoms of pain.

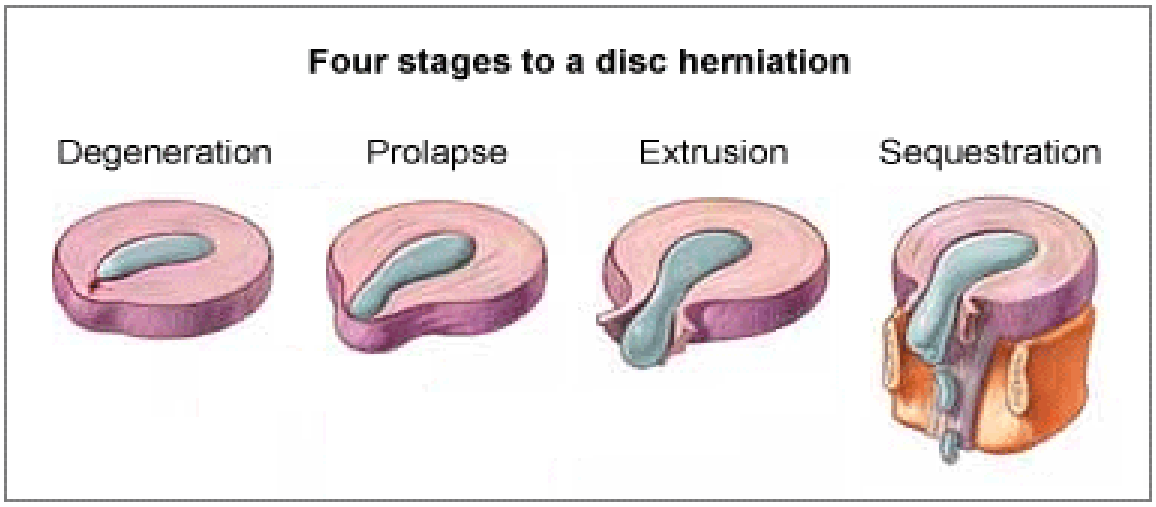

Figure 2: Stages of Disc Herniation (IVDH)[30]

There are four stages of IVD herniation as seen in **Figure 2**: Stage 1) Annular tear: IVD is intact, but a small tear in the outer layer (without herniation), Stage 2) Prolapse: the form of position of the IVD changes with some slight impingement into the spinal canal (i.e. bulge or protrusion), Stage 3) Extrusion: the gelatinous core of the NP breaks through the collagen sheets of the AF but remains within the IVD, Stage 4) Sequestration/Sequestered Disc: the NP breaks through the AF and lies outside the IVD in the spinal canal.[31] The most frequently affected IVDs via IVDH are IVDs with the most substantial range of motion and/or axial loading forces: L3-4, L4-5, L5-S1.

IVDD is a prevalent musculoskeletal disease seen through the aging population. IVDD occurs via a multifactorial process that results in biochemical degradation of NP tissue, a decrease in IVD height, a decrease in IDP, and loss of mechanical function. IVDD is linked to multiple factors in the initiation and progression of the disease: aging, poor nutrient supply, loading conditions, and hereditary factors.[32–38] Consistent IDP changes of the NP result in assuage of the posterior AF. This is identified as part of the aging process

after 45 years of age, thus resulting in total annular lamellae disorganization by the age of 80.[39,40] A research study showed through magnetic resonance imaging (MRI) 20% of patients tested over 45 years of age have an IVD bulge or IVDD, and nearly 60% of patients over 65 years of age had IVDD.[41]

IVDD is a loss of both hydraulic and viscoelastic properties of the IVD through 1) a decrease in the water content and, therefore, a reduction of the preloading effect of the NP, 2) a decrease in the elastic collagen tissue in the annulus with replacement of large fibrous inelastic bands, and 3) cartilage degeneration in the endplates.[29] IVDD is characterized by changes identified in the cellular microenvironment, loss of proteoglycan, loss of IVD height, tears of AF tissue, spinal stenosis, herniated discs, neoinnervation, hypermobility, and inflammation.[42–45]

Degeneration is diagnosed on a grading scale of 0-4 of the IVD (**Figure 3**)and can be referred to the degeneration of the facet joint: Grade 0) no changes in the physiological IVD, Grade 1) joint space narrowing, Grade 2) narrowing in addition to sclerosis or hypertrophy, Grade 3) severe osteoarthritis in addition to beginning narrowing, sclerosis, and osteophytes, and Grade 4) advanced osteoarthritis in conjunction with hypertrophy, narrowing, sclerosis, and osteophytes.[46]

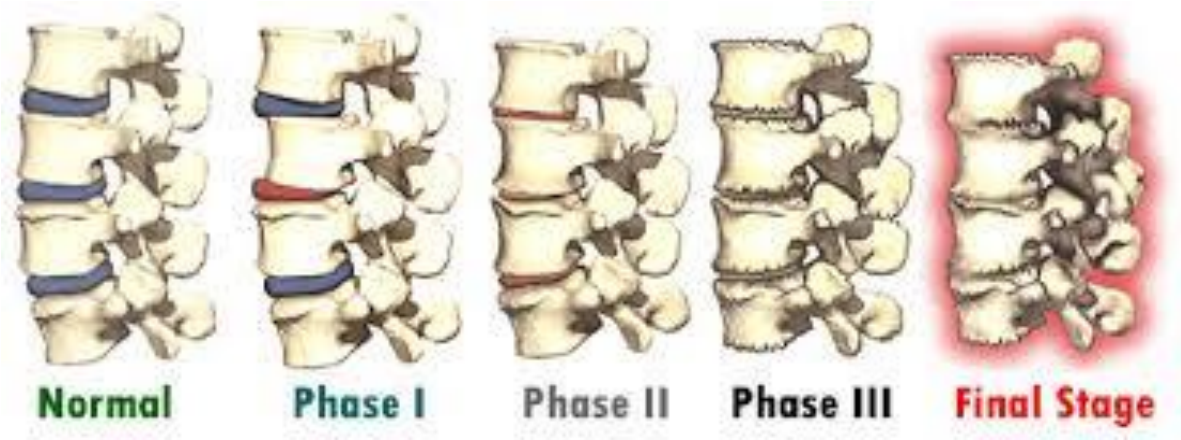

Figure 3: Stages of Disc Degeneration (IVDD)[47]

The level of degeneration has a correlating effect on the amount of IDP observed by the IVD. The mean IDP showed a statistically significant difference between each grade of degeneration, with IDP reduced with increasing levels of degeneration.[48] The IDP in the L4-L5 IVD measured in a patient with a grade 0 degeneration presented a mean of 0.091 [MPa] while a patient with a grade 4 degeneration displayed a mean IDP of 0.010 [MPa].[48]

CURRENT TREATMENTS OF INTERVERTEBRAL DISC DISEASES

Treatment plans for LBP are dependent on the patient's history and the type/severity of pain. Until recently, clinicians believed pain due to herniation would resolve on its own without surgical intervention (i.e. spontaneous resorption of the herniation). However, despite a temporary reduction in pain, a recent study showed that when herniation's are not treated, a resurgence of the pain does in fact occur. The study investigated the course of LBP in a general population of 2000 people aged 30-50 years over a five year period. The study found that for more than 33% of people who experienced

LBP, the pain lasted for >30 days, and out of these 33% of patients, only 9% were pain-free five years later.[49]

The treatment method utilized by a physician is often dependent on the type of injury of the patient, with IVDD and IVDH requiring different treatment approaches. IVDH treatments typically begin with bed rest, NSAIDs, and pain-medications. Sometimes physical therapy (PT) may also be prescribed to improve the patients' symptoms. However, if symptoms persist, epidural injections of corticosteroids to reduce the nerve irritation and facilitate healing may be assessed. If a patient is not responding to 6-12 weeks of conservative conventional treatments, surgical intervention is often considered. For patients suffering from LBP, a microdiscectomy, and/or laminectomy may be performed. Within the United States, (U.S.) lumbar discectomy is the most frequently completed procedure to repair an IVDH, with over 300,000 operations performed annually.,[50] with an associated direct cost of approximately $3,445 per case.[51]

The surgical approach to a discectomy procedure, "minimal or aggressive," is based on the surgeons' personal preference. Both techniques have favorable and unfavorable results, pros and cons. The objective of the surgical procedure, to be considered a complete success, provides the maintenance of the patients' IVD height, and experiences low reoccurrences of IVDH. By maintaining the patient's IVD height, this provides better patient outcomes. A "minimal" discectomy maintains the IVD height, but is at an increased risk of reherniation. While an "aggressive" discectomy reduces the reoccurrence of herniation's, it is linked with IVD height collapse.[52–54] In both surgical approaches, there is the partial removal of the protruding herniated NP tissue and decompression of the neural

elements. During the procedure, a laminotomy/laminectomy, a small piece of the vertebrae removed, may need to be performed to provide access to the herniated fragments. This laminotomy permits a more advantageous visualization for the surgeon of the herniated fragments of the IVD. Consequently, by removing the herniated IVD fragments via discectomy, an open pathway (defect) remains through the layers AF, which provides a path of least resistance for recurrent herniation's to occur. Regardless of surgical approach, an average IVD height loss of 25% has been reported after a discectomy, which is associated with increased back pain and disability.[50] Various studies have shown that reoperation rates range from 9-25% at 4 and 10 years post-operatively,[55–59] which results in direct costs ranging from $2.5k for conservative management to 35k for surgical re-intervention, respectively per case.[60,61] It is imperative to express, current discectomy procedures are not directed to treat the damaged IVD, but rather to alleviate patients' symptoms that may result in further aggravation of existing damage.[10,62,63] Since discectomies are still the most performed spinal surgical procedure worldwide and mainly affects the employed population, the resulting socio-economic consequences are significant.[64]

Alternatively, IVDD is often managed with over-the-counter pain medications (i.e. NSAIDS), and applying ice/heat to the affected area. More aggressive treatments include physical therapy (PT), chiropractic manipulation, electrical stimulation, massage, and last surgery. With surgical interventions, surgical treatments of IVDD are focused towards treating symptoms experienced by the patient rather than restoring native structure and function.

Currently, two IVDD surgical procedures are performed: spinal fusion and total disc replacement (TDR). Both procedures have an objective to preserve the IVD height as seen in **Figure 4**. The traditional procedure, often considered as the "gold standard" surgical treatment, for an IVDD, is the generation of a bony fusion between two vertebral bodies to reduce spinal instability and minimize pain.[65] Shortcomings of a fusion procedure include adjacent segment degeneration and other complications; thus, it is typically employed as a last resort option. Spinal fusions are approached from either the posterior or anterior position. While historically the posterior approach has been used, the anterior approach allows the surgeon to leave an IVD space that more likely will result in the patient having greater pain relief.[66] The cost of spinal fusion typically ranges between $80k to $150k per case; a significantly greater cost as compared to a discectomy procedure.

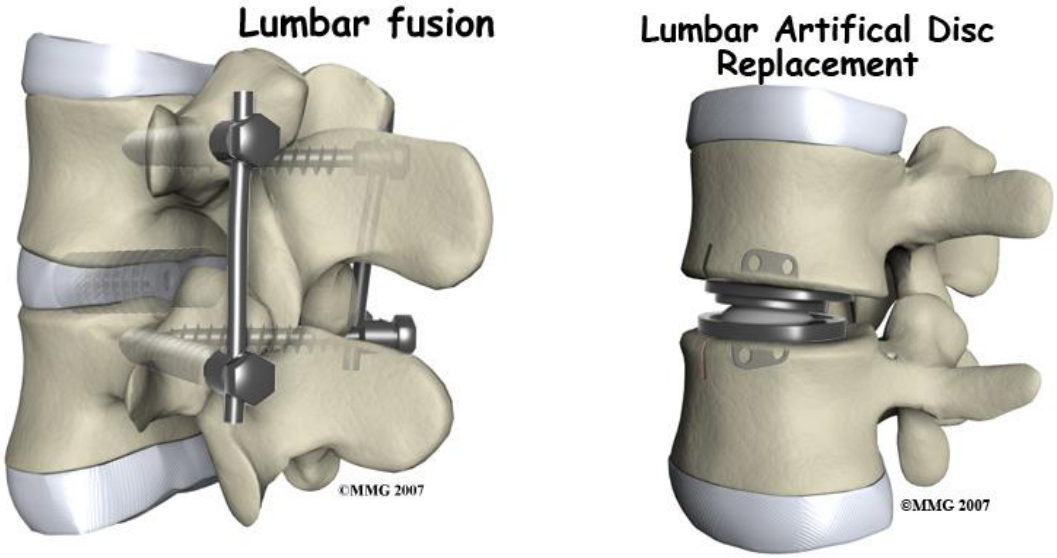

Figure 4: IVDD End-Stage Devices Used for Surgical Repair.[67] Left) Lumbar Fusion Device. Right) Lumbar Artificial Disc Replacement

The more contemporary surgical procedure, TDR, consists of the removal of the damaged IVD, but maintenance of motion is achieved by the use of a prosthetic implant.

However, during a TDR only one of the three joints of the vertebra is replaced, thus limiting the range of motion.[68] Long-term clinical data is still needed to validate the efficacy of TDR.[69] Due to adjacent segment disorders seen with spinal fusions and lifetime of TDR devices revision surgery is an important factor that must be addressed with these clinical procedures. Clinical outcomes have shown that patients undergoing revision fusion surgery exhibited significantly higher rates of unfavorable discharge, prolonged length of stay at the hospital, high-end hospital charges, neurologic complications, pulmonary embolism, wound infections, wound complications, and gastrointestinal and respiratory complications.[70]

REPAIR OF THE IVD

With the short-term lifespan of mechanically assisted devices and limitations of patient's mobility, repair and/or regeneration of the IVD is needed to restore it to its healthy native state. A functional AF must be capable of withstanding the mechanical static and dynamic tensile, burst, and impact loading saw in a healthy IVD. To accomplish this ideology, it is advantageous and obligatory to have an intact AF to allow for native physiological and functional capabilities.

Current surgical procedures for IVDH and IVDD are palliative and suffer from drawbacks. Depending on the amount of herniated material removed, patients undergoing discectomy can be at an increased risk for re-herniation.[55,59] Treatments for IVDD, as stated above, are end-stage surgical interventions that could benefit from an early stage solution, such as nucleus arthroplasty. Current research is being conducted on developing an artificial NP, which would be used for replacing the degenerated native material; however,

the defect in the AF would remain after implantation and migration, respectively. Therefore, in both clinical scenarios it would be advantageous and obligatory to have an intact AF to prevent re-herniation. Accompanying techniques that treat the damaged AF are now increasingly recognized as mandatory to prevent re-herniation, to increase the potential of NP repair, and to confine NP replacement therapies that target early-stage IVDD and IVDH.[71]

These shortcomings and drawbacks of current surgical procedures constitutes a need in which the tissue engineering discipline may be applied to repair the native IVD.

ANNULUS FIBROSUS STRUCTURE

The AF is comprised of circumferential exterior sheets (lamellae) comprised of collagen type I and is an essential constituent of the intervertebral joint. The AF is divided into three layers: peripheral, intermediate, and inner segments. The annulus fibers are found to be thicker and more numerous anteriorly than posteriorly while the posterior fibers express a more parallel alignment.[29] The bundles of fibrous cartilage (multi-layers) runs obliquely from one vertebral body to the next to anchor the IVD to the cartilaginous endplates. The formation of the AF begins at the mesoderm germ layer, one of the three primary germ layers in the early stages of embryonic development. The middle embryological germ layer, mesoderm, forms the mesenchyme that during embryogenesis develops the AF.[72] The composition of the AF is comprised of four main elements: water, collagen, proteoglycans, and non-collagenous proteins. The physiological classification by percentage of these elements is as follows: water (65-90%), collagen (50-70% dry weight), proteoglycans (10-20% dry weight), and non-collagenous proteins (i.e. elastin) (5-25%).[73–

[75] Within the internal portions of the AF, the layers are less hydrated than the NP and more widely dispersed in comparison to the exterior region of the AF.[76] The interior AF also consists of a more substantial amount of GAGs in comparison to the exterior region of the AF: aggrecan and versican.[77–81] Small proteoglycans are found in greater amounts in the internal region: biglycan, decorin, fibromodulin, and lumican.[82–84] The distribution of type I and II collagen also fluctuate based on location within the AF. The exterior lamellae consist purely of type I collagen, but as you move interiorly toward to the NP, overall type II collagen percentage increases as type I collagen percentage decreases. The internal AF is mainly composed of type II collagen, although other collagen types such as III, V, VI, IX, and XI were detected within the inner AF.[85]

The highly organized structure of the AF results in a complex anisotropic behavior, with tensile, compressive, and shear properties differing in the axial, circumferential, and radial directions.[74,86,87] The AF is comprised of collagen sheets (lamellae) with approximately 15-25 lamellae, per IVD,[27] which the fibers are aligned in alternating patterns of $\pm$ 30° to the horizontal axis of the spine, as seen in **Figure 5**.[28]

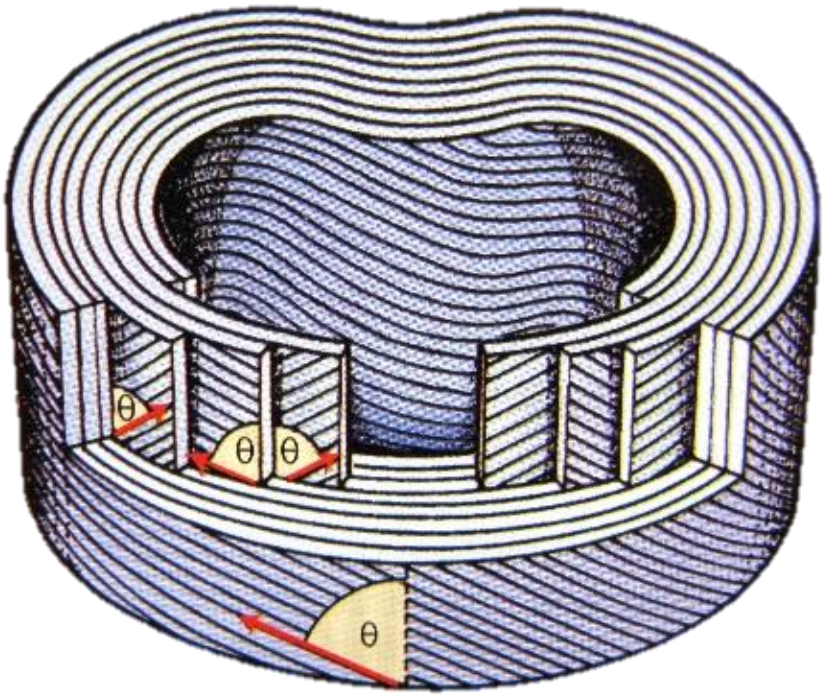

Figure 5: Annulus Fibrosus Lamellae. Arranged in alternating patterns between subsequent layers.[88]

The composition of the lamellae is filled with proteoglycans and interspersed with elastin fibers.[89] In the exterior AF, long elastic fibers are present within the lamellae, running parallel to each other in the same direction as the collagen sheets. However, within the internal AF, the elastic fibers are present between adjacent lamellae as well as increased regular organization within the lamellae.[90] The spaces located between the separate layers of the AF are called interlamellar septae, and they contain proteoglycan aggregates, and a complex structure of linking elements creating interlamellar cohesion.[73,91,92] The ends of the collagen sheets run obliquely from one intervertebral body to the next to attach/secure the IVD to the endplates.

MECHANICAL PROPERTIES OF NATIVE ANNULUS FIBROSUS

Mechanically, the interior AF region is subjected to higher IDP generated from the NP as opposed to higher tensile forces exerted on the exterior region.[93,94] Together these fiber networks couple adjacent lamellae together allowing them to work co-operatively during dynamic loading and prevent separation of lamellae during torsional compressive loading.[95]

The posterolateral location of the AF experiences the highest frequency of layer interruption from various mechanical forces.[96,97] This region is also where the highest stresses are observed during loading,[98] and where annular tears, fissures, protrusions, extrusion, and/or sequestrations are known to develop.[99] **Table 1** illustrates the mechanical characteristics of the native AF.

Table 1: Mechanical Characteristics of the Native AF Tissue

Property	Value
Dimensions L4/L5 IVD	IVD Width: 30.4 ± 4.5 mm[100] NP Width: 19.3 ± 2.9 mm[100] Anterior AF: 20.5% (total IVD)[100] Posterior AF: 15.6% (total IVD)[100]
Burst Strength	Slit (6 mm vertical): 0.93 [MPa][16] Circular Opening (3 mm): 0.64 [MPa][16]
Ultimate Tensile Strength	Anterior: 1.7 ± 0.8 [MPa][101] Posterior: 3.8 ± 1.9 [MPa][101]
Elastic Modulus	Anterior: 7.2 ± 3.1 [MPa][101] Posterior: 27.2 ± 10.2 [MPa][101] Overall 12-24 [MPa][102]
Tensile Fatigue	1043 cycles at 2.3[MPa][101] 10,000 cycles at 1.7 [MPa][101]

HEALING POTENTIAL OF THE ANNULUS FIBROSUS

To unlock the potential for AF regeneration, the native healing potential needs to be addressed. The intrinsic capacity of the AF to cope with damage or degenerative pathological changes have been studied in several animal trials.[103–112] Key and Ford studied the healing capacity of three different types of posterior annulus lesions in a canine model: square annular window, transverse incision, and puncture with 20 gauge needle (0.91 mm).[107] During post-operative procedures, the lesions were initially filled with extravasated blood, fibrin, bone, and cartilage debris. These were gradually replaced by a

thin layer of fibrous tissue at later time points (up to 22 weeks). While the larger damaging lesions (window and incision lesion groups) developed slowly towards IVD protrusion, the lesions that were generated by needle puncture revealed nothing irregular and the site of puncture was unidentifiable after 22 weeks. This study was contradicted however using rabbit IVDs as an organ culture model. The needle puncture showed immediate and progressive mechanical and biological consequences that could lead to degenerative modeling if longer time points were observed.[113]

Smith identified the healing process of the AF occurs in three different phases. In the 1st phase, the outer AF begins to heal. This is caused by a proliferative reaction in the fibrous tissue spreading from the lateral parts of the wound to the medial parts. During the 2nd phase changes occur in the inner annular fibers. The lateral parts of the interior AF layers gradually heal by a slow appositional spread in the medial direction. The process normal begins after a few weeks, but can last up to one-year post-operatively. During the 3rd phase, an increase in the number of collagenous fibers found within the NP tissue, which has remained in the AF wound tract, become increasingly dense.[112]

Although many hypotheses has been formed on what leads to the limited intrinsic healing capability of the AF, many contributing factors remain unknown. One of those reasons may be the fact that exterior repairs are not matched, or insulated to the demands of progressive recruitment of fibers to a tensile force.[114,115] Nevertheless, no matter the underlying reason of why, the limited intrinsic healing capability of the native AF negatively correlates with the success rates of discectomies and NP replacement therapies.[71]

ANNULUS FIBROSUS CLOSURE TECHNIQUES

COMMERCIALLY AVAILABLE PRODUCTS

With tissue engineering, medical devices still in the primitive stage, mechanical closure of the AF is the most effective closure technique currently available on the market. It has been proposed that improved annular closure procedures may reduce IVD re-herniation, and reduce the need for spinal fusion. The most straight-forward solution is per operative suturing of the AF defect. However, suturing does not account for missing AF tissue and may not be strong enough to resist changes of the IDP generated by the NP tissue under different loading regimes. Efficacy and efficiency of suturing the AF have been studied by Ahlgren et al. in an animal study of an ovine model. It was reported that sutured IVDs showed a tendency towards stronger healing, but the results were not statistically significant.[103] As the investigation of an AF closure device continues, Johannes Bron states, the clinical durability the eventual arbiter of technological value.[71]

A diversity of medical devices have been designed or are currently being studied to preserve, repair, and reinforce the AF. The following devices are currently marketed for the proposed use in AF closure after a discectomy to reduce the risk of re-herniation. Anulex Technologies, Inc. has developed two devices: Xclose Tissue Repair System and Inclose Surgical Mesh System. Intrinsic Therapeutics developed the Barricaid Annular Reconstruction Device. Lastly, Magellan Spine Technologies, Inc. has developed the Disc Annular Repair Technology (DART) System. **Table 2** illustrates a comparison of AF repair devices currently available on the market.

Table 2: Comparison of AF Repair Devices Currently Available on the Market

Competitors			
Product	**Company**	**Description**	**Limitations**
Barricaid Annulus Closure Device	Intrinsic Therapeutics	Polyethylene Terephthalate and Titanium Bone Anchor	Long-term (>2 years) results showed no significant reduction in reherniation rates. Potential issues with migration of device. Device lacks ability to regenerate and remodel with host tissue
Xclose Suturing System	Anulex Technologies	Polyethylene Terephthalate	In vitro studies demonstrated the Anulex technology was unable to with stand high physiologcially relevant loads. Device lacks regeneration capabiliteis. In vivo studies showed migration, extrusion, and unable to maintain disc space[2]
Inclose Surgical Mesh	Anulex Technologies	Polyethylene Terephthalate	In vivo studies showed migration, extrusion, and unable to maintain disc space[2]
Suture	Various	Nylon, Polyester, PVDF, and Polypropylene.	Technically demanding due to limited space and potential injury to neurological structures.[1] Single sutre low tensile strength.
Disc Annular Repair Technology (DART) System	Magellan Spine Technologies, Inc.	Polyetheretherketone (PEEK)	No studies currently published in the peer-reviewed medical literature to support the efficacy and safety of the DART system, or that it will improve health outcomes for use in individuals for any indication

The Xclose Tissue Repair System received a 510(k) clearance on August 7th, 2006. The Xclose system consists of non-absorbable, synthetic, poly(ethylene terephthalate) surgical sutures modified with toggle anchors. The FDA labeled indications state the system is used for soft tissue approximation in general and orthopedic surgery procedures. The use of an AF repair was later deemed as outside the scope of the 510(k) clearance. The FDA required the manufacturer to submit a premarket approval application (PMA), in conjunction with clinical data from an investigational device exemption (IDE) study. Xclose and Inclose implants are now commercially available for annuloplasty and can be seen as modified sutures with anchors.[9,11]

The Inclose Surgical Mesh System received FDA 510(k) clearance on August 18, 2005. The surgical mesh is comprised of polyethylene terephthalate (PET) monofilament

expandable braided material that is preloaded on a disposable delivery tool inserted through the defect of the tissue, and affixed to surrounding soft tissue with the anchor bands (non-absorbable sutures). It is proposed as an alternative procedure for annular repair, following a discectomy, to re-approximate the compromised tissue of the AF.

These devices however do not address the underlying issue of using sutures to close the AF. Also, sutures and these devices are fully directed to the containment of the NP, but they do not compensate for the loss of annulus material nor reverse the biomechanical changes that have occurred in the damaged AF.

The Barricaid Device received the CE Mark approval for marketing in Europe in April 2009. It has thus far yet to receive FDA 510(k) clearance for marketing in the U.S. The Barricaid consists of a polytetrafluoroethylene (ePTFE) woven mesh supported by a titanium bone anchor. The function of the device is to form a mechanical barrier that closes the annular defect. The device is intended for use in individuals with primary IVDH with large annular defects. It is a commercially available implant used in adjunction to discectomies that fully bridges the defect in the AF.[12] According to the manufacturers' website, "the Barricaid enables surgeons to directly reconstruct the annulus in the region of the herniation."

The DART System received CE Mark approval for marketing in Europe in April 2009. It has yet to receive FDA 510(k) clearance for marketing in the U.S. The device consists of a polyetheretherketone (PEEK) implant that provides closure of the AF. When implanted, it is placed near the central axis of rotation along the posterior edge of the

vertebral body. It is secured in place by the apophyseal ring along the vertebral body load column.

DEVELOPING SCAFFOLDS FOR ANNULUS FIBROSUS TISSUE ENGINEERING

Ideal AF devices used for tissue engineering is to achieve both immediate mechanical stability and to allow regeneration of native tissue over time. Currently, there is a missing link between addressing AF closure techniques and regenerative strategies. Closure techniques primarily focus on restoration of the mechanical integrity of the AF, while regenerative therapies target the engineering of healthy and functional AF tissue. Furthermore, closure techniques offer the clear implantation and fixation strategy; however, regenerative therapies lack the strategies for implantation and fixation that limits their clinical application.[71]

To develop a suitable scaffold for tissue engineering, certain general principles have to be addressed including, biocompatibility, biodegradability, and method of delivery.[116] On the microscale specific requirements for AF scaffolds include: fill and/or repair the AF defect to contain the NP, allow fixation to the surrounding structures (i.e. endplates and/or surrounding AF tissue), allow AF cells (AFCs) (or stem cells) to survive (differentiate/proliferate), synthesize and secrete the native ECM, have the characteristic anisotropic behavior to maintain/restore the mechanical properties of a spinal motion segment, and not irritate or adhere to the perineurium of the spinal cord.[71] **Table 3** highlights the difficulties and challenges in tissue engineering seen within the cells, scaffolds, anatomy, and physiology.

Table 3: Difficulties and Challenges in Tissue Engineering of the AF Reported by Sharifi et. al.[3]

Sources of Cells	• Limited Sources of human cells due to the unavailability of healthy tissue • Biopsies taken from healthy AF do not contain sufficient cells • Risk of damage to AF during biopsy • Difficulty distinguishing inner and outer AFCs • Difficulties in cell culturing. Loss of cell phenotype in 2D cell culture and the requirement for specific media and culture conditions • Lack of suitable cell markers for AFCs • Poor survival of transplanted cells
Tissue-Engineering Scaffolds	• Requirement of anisotropic physical and mechanical characteristics mimicking the healthy AF • Requirements change with extent of IVD degeneration • Limited integration with native AF tissue • Confirmation to the site of implantation that hinders implantation and restricts implant geometry • Provides an aqueous medium for cell survival, while simultaneously maintaining mechanical properties • Need to promote cell attachment and provide signals for normal cellular activity in the AF ECM • Wish for radio-opacity to allow medical follow-up • Method of surgical implantation or injection
Anatomy and Physiology	• Avascularity of the tissue • Limited nutrient transport and waste disposal • Low healing potential • Low cell numbers • Lack of an animal model of the human degenerated IVD

Overall formation of a scaffold is summarized into two classifications: single composition (oriented or non-oriented to mimic the organized native lamellae) or gradient composition to simulate internal and external layers of the AF. A gradient structure would have an external layer enriched in collagen type I, and an internal layer comprised of more

collagen type II to mimic the native structure of the AF. Several other novel suture, seal, and barrier techniques are currently being developed, resulting in an increasing attention at scientific workshops and conferences.[8–15]

POTENTIAL CELL SOURCES FOR ANNULUS FIBROSUS SCAFFOLDS

In current research, as seen in **Table 4**, the cells used in conjunction with the mechanical scaffolds include both stem cells and native AFCs.[117–124] Within the native human AF, mature subjects have a cell density of ~$9*10^6$ cells/cm^3, which is two times greater than the NP.[125] A recent study showed that cells derived from the human AF were able to differentiate into the chondrogenic and adipogenic lineages.[126] This suggests that cells in the AF could be skeletal progenitor cells that could be recruited under pathologic conditions such as herniation. Otherwise, progenitor cells from surrounding tissue might perhaps be capable of migrating into the IVD.[71] However, isolation of the cells retrieved from a human discectomy procedure typically does not allow for division between internal and external AFCs.

Table 4: Cell Types Used for AF Repair in Current Research for AF Repair

Type of Cells
Porcine Annulus Fibrosus Cells
Mesenchymal Stromal Cells (MSCs)
Human Annulus Fibrosus Cells
Bovine Annulus Fibrosus Cells
Porcine chondrocytes
Rabbit Bone Marrow-Derived MSCs (BMSCs)
Rabbit Chondrocytes
Bovine Annulus Fibrosus Cells
Rat Annulus Fibrosus Cells
Ovine Annulus Fibrosus and Nucleus Pulposus Cells
Murine Annulus Fibrosus Cells
Canine Annulus Fibrosus Cells

INVESTIGATED SCAFFOLD DEVELOPMENT

Abundant varieties of scaffolds have been investigated for AF tissue engineering in academic laboratories. With tissue engineering being a new scope of study and associated high development costs, AF scaffolds are being developed mostly in the academic field. Researchers continue to try and create a suitable AF replacement. **Table 5** lists current materials being used with the hope of mimicking either the native AF structure and/or function.

Table 5: List of Scaffolds Investigated for AF Repair

Type of Scaffolds
Biodegradable Glue (HDI-TMC1-PEG200-TMC1-HDI tissue glue)
Alginate-based collagen shape-memory composite scaffolds
Poly(trimethylene carbonate) (PTMC) scaffolds with an elastic poly(ester-urethane) (PU) membrane
Electrospun biologic laminates
Biodegradable shape-memory polymer network prepared by photo-crosslinking poly(D,L-lactide-CO-trimethylene carbonate) dimethacrylate macromers
Expandable scaffold-free neoconstruct
Bioactive poly(L-lactide) (PLLA/TGF) electrospun scaffold
Biphasic whole IVD using silk protein for the AF and fibrin/hyaluronic acid gel for the NP
Biphasic IVD by electrospinning using PCL as the AF and agarose as the NP
Biphasic whole IVD using collagen 1 for the AF and alginate for the NP
Bone marrow-derived MSC sheets and silk scaffolds
Biphasic scaffold using demineralized bone matrix gelation (BMG) as the AF and elastic material based on poly(polycaprolactone triol malate) (PPCLM) as the NP
Porous silk scaffolds
PDLLA (poly($_{D}$-$_{L}$-lactide)/Bioglass composite foam scaffold
Alginate/chitosan hybrid fiber scaffold
Oriented electrospun nanofibrosus scaffolds
Biodegradable poly(1,8 octanediol malate) (POM) scaffold
Polyglycolic acid (PGA) and calcium alginate mesh coated with 1.5% w/v polylactid acid
Atelocollagen honeycomb-shaped scaffold with a membrane seal (ACHMS-scaffold)

In 2015, Vergroesen et al. published a research study on a biodegradable glue for annulus closure. The aim of the study was to investigate the feasibility and biomechanical properties of biodegradable glue for AF repair, using non-degenerated caprine IVDs. The glue consisted of a biodegradable HDI-TMC1-PEG200-TMC1-HDI tissue glue. The ultimate strength and endurance tests were performed using native and punctured IVDs as positive vs. negative controls. Results demonstrated that the biodegradable glue was able to provide a reduction in the risk of herniation; however, the majority of the IVDs (n=9/11)

failed by nucleus protrusion. Before protrusion of the AF occurred the glue demonstrated a trend toward the partial restoration of the native AF ultimate strength. Results of the study showed: 1) the glue partially restores annulus integrity after a puncture, 2) increases the amount of force required to cause nucleus protrusion through the AF puncture occurs, and 3) limits the number of herniation's during ambulatory loading and ultimate strength tests. The use of biodegradable glue for AF repair provides a low-cost method, but the efficacy would need to be evaluated in long-term studies.[127]

In 2015, Guillaume et al. published a research study on enhancing AF cell migration in shape-memory alginate collagen composite scaffolds through in vitro and ex vivo assessment for IVD repair. For this study, collagen was incorporated into alginate-based shape-memory scaffolds. Addressed were the advantages of using alginate or collagen independently, in producing mechanical stability, injectability, and biological activity. I*n vitro* studies demonstrated that performed alginate scaffolds promoted AF cell penetration and preserved the natural cell phenotype. Also, porcine AF and MSC-seeded scaffolds, with the incorporation of collagen, showed to have a beneficial effect on cell proliferation and ECM deposition. The matrix secretion was amplified by the local release of TGF-β3 growth factor compared to those of non-supplemented media. During *ex vivo* experiments, collagen-enriched scaffolds maintained MSC viability and allowed for attachment of endogenous AFCs from the surrounding tissue and showed infiltration into the 3D constructs compared to alginate only scaffolds.[128]

In 2014, Sharifi et al. published a research study on the treatment of the degenerated IVD through closure, repair, and regeneration of the AF. With cell-based therapies to

regenerate degenerated IVDs, mesenchymal stromal cells (MSCs) are more readily available in contrast to differentiated autologous or allogenic cells. One of the difficulties in cell therapy is most transplanted cells will not survive the ischemic conditions immediately after implantation. It was previously demonstrated with transplanted MSCs, 80-90% died within five days after implantation in an osteochondral defect via rabbits, thus using MSCs for IVD treatment seems imprudent.[129] Further addressed were the advantages and disadvantages of cell types for direct transplantation into the degenerated IVD. Autologous NP or AFCs do not initiate an immune response, although they are not available in sufficient amounts, and healthy state, their phenotype change upon expansion in monolayer culture, and additional surgery is required to obtain NP or AFCs with the risk of causing further IVDD upon harvesting. Allogeneic NP or AFCs do not initiate an immune response, and healthy cells are available; although, there is a limited availability of allogenic human NP or AFCs, and there is a risk of IVDD upon harvesting. Autologous stem cells elicit no immune response and are available in sufficient amounts; however, there presents a lack of definitive phenotype markers for NP or AFCs. Allogenic stem cells do not elicit an immune response and have "off the shelf" availability; although, they also lack definitive phenotype markers for NP or AFCs. Lastly, chondrocytes are available in sufficient amounts, but they have a different phenotype compared to NP or AFCs.[3]

In 2014, Pirvu, et al. published a study that included a combined biomaterial and cellular approach for AF rupture repair. The study utilized poly(trimethylene carbonate) (PTMC) scaffolds seeded with bone marrow-derived MSCs in a combination with an elastic poly(ester-urethane) (PU) membrane. The mechanical properties of the PU

membrane showed an ultimate strength of 53.0 +/- 2.0 MPa, and a yield strength of 4.9 +/- 1.4 MPa. The surfaces and cross section showed the absence of large pores and minor amounts of non-connected micro-porosity. Through testing it was demonstrated the PTMC implant combined with the sutured PU membrane restored IVD height of annulotomized IVDs, and prevented herniation of NP tissue into the AF defect. In comparison, press-fitted implants without closure were not able to withstand dynamic loading and were pressed out of the defect immediately after starting loading cycles. The PU membrane sutured onto the AF tissue was used to cover the scaffold and seal the defect. After 14 days of repetitive dynamic load, the sutured PU membrane retained the PTMC scaffold within the AF defect, and no herniation of the NP was observed. Through cellular studies, MSCs showed potential of positively modulating cell phenotype of native IVD tissue by up-regulating anabolic mechanisms and downregulating catabolic mechanisms in host IVD cells. MSCs were implanted into the AF defect by first embedding in fibrin hydrogel. After 14 days of culture, *in situ*, with repetitive dynamic load, the implanted MSCs remained within the PTMC scaffolds. This suggests that implanted MSCs can adapt their phenotype during culture within IVDs.[130]

In 2013, Guillaume et al. published a research study on shape-memory porous alginate scaffolds for regeneration of the annulus fibrosus and the effect of TGF-β3 supplementation and oxygen culture conditions. The porous shape-memory alginate scaffolds were structurally based on covalently cross-linked alginate. Manual manipulation of the scaffolds exhibited shape-memory capability suitable for delivery in AF defects of the IVD through minimally invasive approaches. The scaffold was developed as a support

template for AF cell proliferation and tissue formation. *In vitro* testing demonstrated cytocompatibility when seeded with porcine AFCs and supported cell penetration, proliferation, and ECM deposition when cultured in IVD like micro-environmental conditions (low oxygen and low glucose concentrations) with TGF- β3 media supplementation. With TGF- β3, after three weeks of culture sulphated GAG (sGAG) and collagen type I were detected throughout the entire porous network of the alginate scaffold. Without TGF-β3, cells agglomerated in small clusters with limited proliferation which resulted in poor ECM deposition. It was also stated that cells did not appear to attach directly to the alginate structure itself. Guillaume believed this to be due to the low cell adhesion properties of alginate, and to mimic the natural orientation of collagen fibers in engineering scaffolds, various fabrication methods and specific architectures have been investigated previously. These structures could potentially be incorporated into the alginate solution before cross-linking to create a composite alginate-based porous scaffold with aligned fibers.[131]

In 2013, Driscoll et al. published a research study on biaxial mechanics, and inter-lamellar shearing of stem cell seeded electrospun angle-ply laminates for AF tissue engineering. The study focused on electrospun biologic laminates reaching biaxial properties of the native tissue. It was found that properties of the opposing ($\pm$ 30°) constructs were significantly higher than the aligned constructs despite showing similar fiber stretch ratios. This could indicate that a lamellar structure with native tissue fiber orientation can provide higher stiffness than a single aligned fiber population, due to biaxial boundary conditions. It is stated that the use of biaxial testing is necessary for an

appreciation of this difference since previous uniaxial tensile testing showed single lamellar 0° constructs to be about twice as stiff as opposing constructs. This provides further evidence that a lamellar structure with two alternating or angle-ply fiber populations is an important design criterion for both native tissue and a mechanically functional engineered AF. The limitation of the electrospun angle-ply laminates was found to be the strain levels. Native AF function under large strains without failing and typical have highly nonlinear mechanics with large toe regions. The electrospun biologic laminates displayed a nonlinear response to strain, although at a lesser extent and with a smaller toe region than the native tissue.[132]

In 2013, Sharifi et. al. published a research study on an AF closure device based on a biodegradable shape-memory polymer network. The biodegradable elastic polymer network was prepared by photo-crosslinking poly(D,L-lactide-CO-trimethylene carbonate) dimethacrylate macromers. The mechanical properties of the scaffold were reported in the range of native human AF tissue for tensile strength, elastic modulus, and elongation at break. The cell culture of human AFCs (HAFCs) showed good cell adhesion and proliferation. Cell culturing studies were evaluated on network specimens that were either pre-coated or not-coated with fibronectin. Fibronectin was utilized because it is previously reported as an ECM protein that improves cellular adhesion on a polymer surface. The feasibility of the shape-memory device was evaluated using a cadaveric canine model. Upon insertion into the IVD, the device had begun to deploy. It was reported that the network samples had a shape-recovery rate of 9.3% per minute when heated at a rate of 2° C per min. After overnight incubation at 37° C, the IVD was cross-sectioned. It was found

that the implant recovery to its permanent shape was not complete. This was believed to be due to the shape-recovery force of 1 MPa not being larger than the force exerted by the surrounding AF tissue on the implant. Also, through manually applied flexion and extension forces, and axial rotations the implants dislodged from their original positions. Thus, it is necessary for an improvement in the design of the implant to increase the mechanical properties needed to withstand native forces.[133]

In 2013, Cho et al. published a research study on the construction of a tissue-engineered AF. In this study, they characterized an expandable scaffold-free neoconstruct using autologous AFCs. The construct was prepared from pellet cultures, derived from monolayer cultures of AFCs from mature pigs, until the cells had reestablished a proteoglycan rich cell associated matrix. The second step consisted of the removal of the cells embedded in their own ECM products as a membrane from culture plates and subsequent maintenance as a detached explant tissue. This method consisted of using only the matrix produced by the cells themselves and does not require the use of exogenous matrices. The collagen content and biomechanical properties after three weeks of culturing was similar to that found in mature porcine AF tissue. The principle advantages of these constructs observed were the artificial materials are not required to obtain a sizable 3D AF tissue construct, and the cell distribution was uniform. This contrast could provide applications for analysis of cell behavior as it provides a well-defined 3D environment for studies of biomechanical load or growth-factor stimulation.[134]

In 2012, Vadala et al. published a research study on bioactive electrospun scaffolds for AF repair and regeneration. The scaffold was synthesized by electrospinning, with a

direct incorporation of TGF-β1 into the polymeric solution. The scaffold was a poly(L-lactide) (PLLA/TGF) electrospun scaffold. The electrospun scaffold consisted of a non-woven porous mesh with randomly oriented fibers. The study demonstrated a sustained release of growth factors and inducement of anabolic stimulus on bovine AFCs while mimicking the ECM three-dimensional environment of the AF tissue.[135]

In 2012, Chan et al. published a research study on IVD regeneration or repair with biomaterials and stem cell therapy, and if it is feasible or fiction. They describe how commercially available implants for closing the AF reinforces the complete posterior annulus and could prevent contralateral herniation. Although, these devices are unable to maintain the biological AF structure in the long-term or stop AF degeneration. Tissue engineering methods aim to close the injured AF to prevent IVDH as well as to stop the AF from further degeneration. They also identified the previously attempted engineering approaches, such as hydrogels, alginate, PDLLA/Bioglass, silk, and electrospinning discussed further in this paper. Additionally, a whole IVD tissue engineered total disc replacement was addressed: A biphasic whole IVD using silk protein for the AF and fibrin/hyaluronic acid gel for the NP using porcine AFCs and chondrocytes respectively. Another approach described was a fabricated biphasic IVD by electrospinning using PCL as the AF and agarose as the NP. Lastly, the last approach addressed was a biphasic whole IVD using collagen 1 for the AF and alginate for the NP. An issue they address is the major challenge of not de-differentiating cells in culture after in vitro culture. With primary cells starting to dedifferentiate when they are cultured in vitro over long passaging ($p>6$),

strategies are needed to control the state of the cells to ensure these cells are not de-differentiated over long expansion time and remain suitable for IVD tissue engineering.[136]

In 2012, See et al. published a research study on simulated IVD-like assembly using bone marrow-derived MSC sheets and silk scaffolds for AF regeneration. The structure used to form the IVD-like assembly was constructed of a cylindrical silicone NP substitute. The study addressed the potential to regenerate the AF by using rabbit bone marrow-derived MSCs (BMSCs) to form cell sheets and incorporating them onto silk scaffolds. The study demonstrated that BMSC cell sheets can be successfully transplanted and adhere well when combined with silk scaffolds. The cells within the assembly remained viable and showed the presence of GAGs throughout the ECM. Through immunohistochemical (IHC) staining, collagen type I and II were present and the composition of type II increased from 8% to 70% over a four week culture. This could prove this method has potential to regenerate ECM similar to that of the internal AF. One shortfall of the study was no specific markers or genes to are known to differentiate the IVD cells from other lineage-specific cells. However, due to the lack of specific markers, studies have only reported that the internal and external AF have a gene expression profile and ECM that resembles those synthesized by articular chondrocytes and fibroblasts, respectively.[137]

In 2008, Wan et al. published a research study on a biphasic scaffold for AF tissue regeneration. In this study, a biphasic scaffold was used to simulate the annulus both structurally and elastically. They describe the generation of a cylindrically shaped composite implant designed to emulate the AF. The outer phase of the scaffold consisted of demineralized bone matrix gelation (BMG). The inner phase of the scaffold was

constructed of an elastic material based on poly(polycaprolactone triol malate) (PPCLM). The BMG phase was used to increase the mechanical strength and to simulate the ligamentous structure of the outer AF. The PPCLM phase was seeded with rabbit chondrocytes that showed proliferation and ability to maintain their phenotype with a four week culture.[123]

In 2008, Chang et al. published a research study on enhancing AF tissue formation in porous silk scaffolds. This study was an extension to their previous publication, "Porous Silk Scaffolds to be used for Tissue Engineering." The aim of this study was to determine whether dynamic culture and/or scaffold pore size would influence AF tissue formation and distribution in silk scaffolds *in vitro*. It was shown that scaffolds with an average 600 μm pore size appeared to be the best model to mimic the native AF. Scaffolds were seeded and grown in either static culture or spinner flasks (90 rpm). After two weeks, scaffolds in the dynamic culture showed greater than 3-fold increases in collagen accumulation per cell compared to static cultures, and a 1.5-fold increase per cell in proteoglycan accumulation. The tissue generated under dynamic conditions also appeared to be more cellular as the DNA content was significantly greater compared to static cultures. However, in both the static culture and spinner flasks the scaffolds had a similar pattern of tissue distribution as more tissue was present on the outer surface, with little tissue formation on the interior of the scaffold.[138]

In 2008, Helen et al. published a research study on cell viability, proliferation, and ECM production of HAFCs cultured within PDLLA/Bioglass composite foam scaffold *in vitro*. The scaffolds were comprised of poly(D, L-lactide) (PDLLA)/Bioglass. The PDLLA

composite foams were combined with varying percentages (0, 5, and 30 wt.%) of Bioglass through thermally induced phase separation (TIPS), and characterized by scanning electron microscopy (SEM). HAFCs were used to determine viability, cell attachment, proliferation, and proteoglycan/collagen production. Live/dead staining showed viable HAFCs were present on the top surface of the foams as well as penetrating into the internal pore structure. SEM observations revealed larger quantities of clusters of HAFCs were attached to the pore walls to the foams with 5 and 30 wt.% Bioglass in comparison to the 0 wt.% Bioglass. DMMB assays showed HAFCs cultured within the PDLLA/30BG foam had a greater ability to deposit collagen and proteoglycan after four weeks of culture compared to lower wt.% Bioglass. IHC analysis of collagen production demonstrated that collagen produced in all cultures was predominantly type I collagen, similar to collagen found in the external AF.[122]

In 2007, Chang et al. published a research study on porous silk scaffolds to be used for tissue engineering. The biomaterial used was a protein polymer made by silkworms, silk fibroin. The idea that the use of a silk scaffold would potentially degrade at a sufficiently slow rate would allow for proper tissue development, and could be covalently coupled to peptides to allow for the potential of enhancing cell attachment. The results of the study demonstrated that AFCs adhered to porous silk scaffolds and synthesized collagen and proteoglycans after attachment: with a 10-fold increase in collagen deposition and a small increase in proteoglycan content. After 24 hours, 35% cells seeded into the scaffold had attached, but only a significant increase in cellularity was observed on day 56. However, with the coupling of RGD-peptides, there was no evidence of further cell

attachment, collagen accumulation, or tissue formation. RGD decoration showed to have no effect on cell seeding efficiency or morphology. The silk fibroin scaffold was found to be a suitable scaffold material for AF tissue engineering; however, it was observed that tissue growth was limited and not uniformly distributed throughout the scaffold.[118]

In 2007, Shao et al. published a research study on developing an alginate/chitosan hybrid fiber scaffold for AFCs. The study utilized a fibrous scaffold made of alginate or alginate/chitosan created by wet-spinning and lyophilization. Demonstrated through testing, alginate/chitosan hybrid scaffolds exhibited a slower degradation rate than pure alginate fiber scaffolds while both scaffold types did not display any cytotoxicity to 3T3 fibroblasts and could maintain canine AFC growth. Cellular studies showed AFCs retained their spherical shape within the fibrous scaffold at the beginning of the culture period and formed into cell aggregates at later time points. ECM molecules, including collagen I and II, aggrecan deposition were also detected in the AFC clusters.[117]

In 2007, Nerurkar et al. published a research study on the mechanics of oriented electrospun nanofibrous scaffolds for AF tissue engineering. The study utilized electrospun poly-ε-caprolactone nanofibrous polymer scaffolds. Bovine AFCs were seeded onto the scaffolds, and biochemical analysis was performed on days 1, 14, 28. The model was used in contrast against single lamellae of the native internal and external regions of the AF. Results demonstrated elongated cells aligned along the predominant fibers direction with proteoglycan (s-GAG) and collagen content increase over the four week culture. Uniaxial tension mechanical testing was performed on various fiber angles of the scaffold: 0°, 15°,

30°, 45°, and 90°, and showed that moduli varied nonlinearly between the different fiber angles. A nonlinear decrease in modulus was seen with increasing fiber angles.[120]

In 2007, Wan et al. published a research study on a novel biodegradable poly(1,8 octanediol malate) for AF regeneration. The scaffold was formed using malic acid-based polyester poly(1,8 octanediol malate) (POM), which was synthesized by direct polycondensation. Tensile strength, compressive stress, and compressive Young's modulus of POM demonstrated an increase with the extension of the polymerization time of POM. However, degradation rates and elongations of POM decreased with extensive polymerization of POM. Rat AFCs were seeded onto the scaffold and showed that AFCs did not attach readily to the polymer after polymerization times less than two days. Rat AFCs were then cultured in monolayers for 1, 2, and 4 days. As time points increased, proliferation of cells with stellate and elongated morphology was seen, with an increase in gene expression for aggrecan and type II collagen only seen on day 4.[121]

In 2007, Wan et al. published a research study on a biphasic scaffold for AF tissue regeneration. They created a biphasic elastic scaffold comprised of an inner and outer phase sections. The outer phase was a ring-shaped demineralized BMG extracted from cortical bone. The BMG was studied due to its ECM composition of mainly type I collagen, its natural biomechanical properties, and because it contains insoluble bone morphogenetic proteins, non-collagenous proteins, and intrinsic growth factors. The inner phase was a bio-biomaterial poly(polycaprolactone triol malate) (PPCLM) orientated in concentric sheets and seeded with chondrocytes. Mechanical testing was conducted on the scaffold to test for the incorporation of BGM into the PPCLM scaffold. Through testing, it was found that

mechanical properties and degradation of PPCLM could be adjusted by controlling the post-polymerization time of the pre-polymer. Mechanical testing results demonstrated good biocompatibility in foreign body response *in vivo* assay, enhanced compressive strength and 50-fold greater tensile stress. Rabbit chondrocytes were seeded onto the scaffold and showed proliferation and penetration into the inner phase after four weeks. Production of type II collagen and aggrecan was detected in both phases of the scaffold.[123]

In 2006, Helen et al. published a research study on the potential use of PDLLA/45S5 (PDLLA-poly($_{D}$-$_{L}$-lactide))/Bioglass composite films for the culture of AFCs *in vitro*. The study evaluated the attachment and matrix production of bovine AFCs to four different substrates. They chose to combine bioactive glass with degradable polymers due to the ion dissolution products of the bioactive ceramic counteract the acidic degradation products of the polymer to reduce the inflammatory response. Through SEM analysis it was shown that cells had attached and spread on all films after three days and had proliferated to form a confluent monolayer of cells by day 7. sGAG production was measured, and shown that PDLLA/30BG had enhanced sGAG production after three weeks; although, after four weeks in cultures sGAG production decreased. The results of the study showed that PDLLA/Bioglass provided an appropriate substrate for AFCs and that these films promote the production of an ECM containing abundant sGAG and collagenous proteins.[139]

In 2004, Mizuno et al. published a research study on tissue-engineered composites of the AF and NP for IVD replacement. The study used a polyglycolic acid (PGA) and calcium alginate mesh coated with 1.5% w/v polylactic acid solution. AF and NP ovine

cells were seeded onto PGA and alginate scaffolds to create a tissue with AF and NP components. Based on histologic and biochemical characteristics of the tissue-engineered IVDs, they presented similar to those of native IVDs based on morphology and quantities of collagen and proteoglycans produced. DNA content remained constant during first eight weeks but increased greatly between 12-16 weeks *in vivo*. Amounts of hydroxyproline and GAG increased with time with GAG reaching native tissue levels after 16 weeks.[119]

In 2002 and 2003, Sato et al. published research studies on an atelocollagen honeycomb-shaped scaffold with a membrane seal (ACHMS-scaffold) and the regeneration of the IVD with an allograft of cultured AFCs. During manufacturing, it was found the diameter of the pores could be controlled by changing the concentration of collagen solution and ammonia gas. The first study demonstrated stability, cytocompatibility, uniform seeding of cells, and accumulation of produced matrix components within the ACHMS-scaffold. The objective of the second study was to investigate the regeneration of IVDs after laser discectomy using their tissue engineering methods. They used AFCs isolated from Japanese white rabbits and seeded them onto the ACHMS-scaffold for one week. They then implanted the scaffold into the lacunas of an IVDs of recipient rabbits that had the NP vaporized by a laser. Results demonstrated cells proliferated and retained spherical shape, higher increases in type II collagen and GAG content than compared to monolayer content, and a presence of accumulation of cartilage-like matrix after insertion.[124,140]

TISSUE ENGINEERING AND REGENERATIVE MEDICINE

Tissue engineering evolved from the field of biomaterials and refers to the combination of scaffolds, cells, and suitable biochemical and physicochemical factors to form functional tissues to improve/replace biological functions. There is a need to create an effective AF repair device with could improve patient outcomes and reduce healthcare costs while preventing re-herniation and the need for spinal fusion for patients with IVDH and IVDD, respectively. Regeneration of the damaged AF is an appealing concept since it permits restoration of all functions of the AF; however, this concept is exceptionally complex to attain. It must be able to endure the direct mechanical strength applied and be a size sustainable to contain the NP.[141] The progression in development needed for the success of regenerative strategies of the AF consists of three major components: cell therapy, gene therapy, and scaffolds.[63] Proclaimed in a recent study, the ideal strategy for IVD regeneration is to restore the function and integrity of the IVD by using biomaterials, native matrices, growth factors, and cells that produce matrices; although, with the complex biological, mechanical environment of the IVD makes the synthesis of an artificial IVD a difficult task.[85] However, while a difficult task, without a functional AF repair device to resist expulsion of NP tissue and the IDP, generated within, IVD regeneration and prevention of IVDD and IVDH is deemed to fail.

During the early 2000's there was an increase in research of NP replacements with the goal of restoration of the physiological IDP and IVD disc height. However, there was a lack of effective strategies that combated the damaged AF (incurred via implantation of such devices or the pathological processes). Current strategies for NP replacements attempt

to restore native NP mechanical properties, but do not address the issue of the inferior quality of the surrounding AF, which is not capable of withstanding IDP.[71] Recently in research, IVD engineering strategies are increasingly focusing on the regeneration or repair of the AF in order to reduce the number of re-herniation's, increase the potential of NP engineering strategies, and to mechanically assist NP replacement therapies.[141,142]

An effective AF closure/repair device in conjunction with a less aggressive discectomy for IVDH and/or NP arthroplasty for IVDD, may result in improving patient outcomes, decreased pain, and provide fewer revision surgeries via lower re-herniation and expulsion rates.[5,6] In either case, an intact AF must be re-established to prevent implant expulsion or re-herniation, thus addressing the two major spinal pathologies directly associated with an IVD. Therefore, it would be advantageous to develop a biomimetic patch for biological augment AF repair to help mitigate this re-herniation.

The objectives of this research were to investigate the development of a biomimetic patch for biological augment AF repair through: (1) characterizing the micro-architecture of the multi-laminate angle-ply AF patch, (2) evaluating the mechanical properties of the developed multi-laminate angle-ply AF patch, and (3) evaluating the cytocompatibility of the multi-laminate angle-ply AF patch.

CHAPTER II

MATERIALS & METHODS

SPECIMEN PROCUREMENT, DISSECTION, AND TREATMENT

Porcine hearts were obtained at time of slaughter from a local abattoir. The parietal layer of the pericardium was separated from the heart, and excess adipose fatty tissue and connective tissue were removed by manual separation using tweezers and scalpel blades. The parietal pericardium layer was chosen due to its natural structure. The parietal pericardium is fused to and inseparable from the fibrous pericardium (most superficial layer of the pericardium). It consists of dense and loose connective tissue containing collagen type I.[143] The dense connective tissue is divided into regular and irregular sections. Dense regular connective tissue contains collagen fibers bundled in a linear/parallel orientation. The presence of these collagen fibers were utilized during fabrication of the scaffold. The decellularization procedure was adapted and modified from methods described by Teeder et al without elastase treatment.[144]

FABRICATION OF BIOLOGICAL COLLAGEN ANGLE-PLY SCAFFOLD

Multi-laminar angle-ply collagen patches were designed to mimic the native architecture of the AF. Angle-ply patches consisted of multiple layers of pericardium tissue adhered together via a sewing machine, backing material, and suture thread (Rachel Reference if previously reported). Single layers of pericardium were placed on a light box to determine the preferred direction of the collagen fibers. The layers were then stacked one on top of the other at $\pm$ 30° alternations to create the native angle-ply formation

(**Figure 7**). For sewing, the layers were placed on top of a water-soluble backing material (solvy-ultra). The backing tissue was necessary during sewing to provide even positioning, and to permit the needle to puncture all the layers of the pericardium. Dimensions of 8 x 8 mm^2 were sewn into the layers to create the multi-laminar angle-ply patch. The backing material was then removed manually by hand/tweezers, and stored in ddH_2O for 4 hours to ensure complete degradation from the patch. The dimensions of a three layer patch are: length (8 mm), height (8 mm), and width/thickness (0.8 mm).

ISOLATION AND EXPANSION OF BOVINE AF CELLS

Three bovine tails from young calves were obtained at time of slaughter from a local abattoir. The caudal discs were separated using mechanical shears, and the NP was removed first through a 6mm biopsy punch in order to ensure harvest of only the AF. The AF tissue was then removed and minced using two scalpel blades. The tissue was then transferred to a 50 ml conical tube with 25 ml of collagenase solution (1% Ab/Am, 0.2% Collagenase Type I (125 units/mg dry weight) and DMEM). Following tissue digestion overnight (~18 hours) at 37°C, the solution was centrifuged at 1000 rpms for 5 minutes. The supernatant was removed and the cells were re-suspended in cell culture media (1% Ab/Am, 10% FBS and DMEM). Passage 2 (P2) bovine AF cells were used in the current study.

CELLULAR ANALYSIS

Cellular studies were conducted on the multi-laminar angle-ply AF patch to ensure cell viability on all layers of the patch. Previous laboratory testing showed that bovine AFCs were viable on the surfaces of the patches through day 15 studies; however, cell

viability between the upper and lower layers was unattainable. Multiple variations of tissue disruption modifications were used with the hypothesis of degrading the tissue matrix to provide more nutrients to the inner layers. For all studies, patches were prepared by re-sterilization and neutralization before cell seeding. Sterilization occurred by placing the patches in a specimen cup with 100 ml of 0.1% Peracetic Acid on a shaker at room temperature for two hours with a speed of 150 rpms. The patches were then washed in 100 ml of sterile PBS for 1 hour (3x) on a shaker at room temperature for one hour with a speed of 150 rpms. The patches were then neutralized in 100 ml of sterile 50% fetal bovine serum (FBS)/ 48 % Dulbecco's Modified Eagle Medium (DMEM) + 2% antibiotic/antimitotic (Ab/Am) overnight on a shaker at room temperature with a speed of 150 rpms. The tissue disruption performed and discussed herein was sonication of the tissue. Pericardium tissue was placed in a Sonicator for 20 minutes prior to patch fabrication. Sonication affected the tissue by pressure created through a probe which rapidly expands and contracts at high frequencies. The high frequency oscillation is due to the piezoelectric effect, with rapid oscillation of the current causing tiny shock waves.[145]

AF CELL SEEDING ONTO SCAFFOLD

Following sterilization and neutralization, patches were divided into 2 separate groups: control and sonicated. 5×10^6 cultured bovine AF cells at passage 2 (P2) were placed in a predetermined amount of cell culture media. Previous studies not shown herein, determined the optimized volume amount to prevent run-off of the patch. 6×10^5 cells were seeded per patch (16×10^3 cells per mm^2): 2×10^5 cells were seeded in 40 µl of CCM onto the top the patches, 2×10^5 cells seeded in 75 µl of CCM were injected into the middle

layers using an 18 gauge needle. The patches were then incubated at 37°C for four hours for cell attachment. After incubation, the patches were flipped using sterile tweezers, and the same process was completed for seeding 2 x 10^5 cells in 40 µl of CCM onto the bottom of the patch.

STAINING HISTOLOGY

Representative samples of single layer decellularized pericardium were aligned in alternating degrees to illustrate the articulation of the alternation of fibers within pericardium tissue. This was performed with the intent to mimic the native angle-ply foundation of the human AF. Patches were fabricated as stated above, in $\pm$ 30° and + 30° alternations. The samples were then analyzed via histological analysis. Representative samples were placed in histological cassettes with gauze to hold the sample in place and to prevent swelling between the layers. The samples were then fixed in neutral buffered formalin for 24 hours, embedded with paraffin wax, and sectioned at 5 µm thickness. Hematoxylin and Eosin (H&E) staining was performed to visualize cellular material and tissue extracellular matrix. Masson's trichrome staining was used to define the composition of the pericardium tissue, and to verify the angle-ply alternation between the layers. A Zeiss Axio Vert.A1 camera microscope with AxioVision SE64 Rel. 4.9.1 software was using for imaging and reviewing of the histological slides.

BIOMECHANICAL EVALUATION OF MULTI-LAMINATE AF PATCH

ULTIMATE TENSILE STRENGTH

Mechanical tensile testing was performed on decellularized single and multi-laminar angle-ply AF patches to ensure comparable tensile ultimate tensile strength (UTS)

to native human AF tissue. This is deemed crucial to ensure the patch does not disrupt the function of the native tissue, and is able to withstand the max tensional force experienced during extension and flexion. The representative samples for the decellularized single layer pericardium were tested in a fiber preferred (tension applied parallel to collagen fibers; n=5) and cross-fiber direction (tension applied perpendicular to collagen fibers; n=5). Representative samples of three layered multi-laminar angle-ply AF patches were also tested (tension applied at $\pm$ 30° alternating angles of patch aligned to the vertical axis; n=5). The tensile testing protocol was adapted from methods describing single human AF lamellae tensile testing by Green et. al.[101]

Testing was performed on a mechanical testing system (MTS) Synergie-100 fitted with a 100 N load cell. Samples were preheated to 37°C in a water bath for 30 minutes prior to testing and sample length, width, and thickness were determined using digital calipers. Samples were placed in tensile grips lined with fine-grit sandpaper to the ends of each sample before insertion into the MTS clamps to prevent slippage. Once samples were secured, preconditioning (5 cycles to 10% stain at 10 mm/min), and testing to failure at a rate of 240 mm/min was performed. Stress strain data was recorded, plotted, and collected for statistical analysis. The tensile elastic modulus was determined from the linear region of the graph. The UTS was determined by dividing the max peak load by the cross-sectional area of the sample.

PATCH IMPACT RESISTANCE

Impact strength was determined in accordance with ASTM D1709 with minor modification. Representative samples of multi-laminar angle-ply AF patches of 1, 2, 3 and

6 layers were tested (n=4 per group). The impact mechanical test was performed to obtain the minimum number of layers required to withstand the changes of IDP of the IVD. Understanding the impact force is crucial due to high rapid changes in IDP which could result in herniation's of weaken or damaged areas of the IVD. The impact force was determined using a custom design sled fixture consisting of four rails attached to a base platform, with a free-moving apex platform. The testing apparatus for the tissue consisted of two wooden blocks bolted together with a 6.25 mm diameter hole drilled through the center of both blocks. On the inner surface of each block a neoprene square glued down with epoxy along with a layer of sandpaper to prevent the samples from slipping during testing. The representative samples were centered over the hole in the block and bolted together. A 6 mm steel ball and rod was slid through the top block and placed in contact with the tissue. The remaining rod extruded from the wooden block towards the apex of the apparatus. Concisely, various weights ranging from 0.18-0.58 kg were dropped from a consistent height of 10 in (0.254m) towards the base of the platform along the four rails. The impact between the weight of the free-moving apex platform and rod were used to measure the amount of force the patch could withstand.

Using the application of conservation of energy of a falling object EQ 1, the impact velocity and kinetic energy were calculated. Thus, combined with the distance traveled, impact force [N] was calculated. In conjunction to the impact force data, the contact radius between the ball and patch was needed in order to convert to pressure. The law of conservation of energy and the following formulas were used to calculate the contact radius:

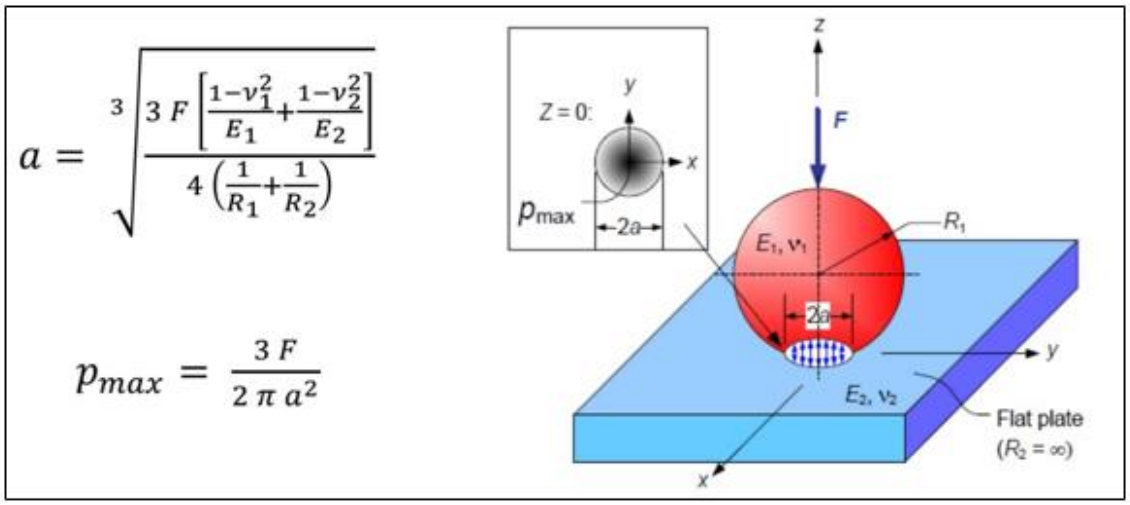

Figure 6: Method of Maximum Pressure Calculations. A sphere on a flat plate (a flat plate is a sphere with an infinitely large radius).[146]

This formula represents the calculated contact surface [m] of the ball with the pericardium. F is the load [N] of the force exerted on the patch at the time of impact. R_1 and R_2 were the radius [m] of the ball (3 mm) and the patch (∞) respectively, where the patch was considered a sphere with an infinitely large radius. E_1 and E_2 were the elastic modulus [Pa] of the ball (200 GPa) and the patch (16.4 MPa, determined from tensile testing), respectively. Poisson's ratios, υ_1 and υ_2, of the ball (0.27) and the pericardium (0.3), respectively.[7–9] Potential Energy (PE) and kinetic energy (KE) were used based on the conservation of energy calculation to determine the impact force of a falling object. Impact force was then converted to pressure [Pa] to relate to IDP changes (EQ. 3). The data was collected and recorded for statistical analysis.

TENSILE FATIGUE TESTING

Mechanical tensile fatigue testing was performed on three layered multi-laminar angle-ply patches to test the ability of the angle-ply patch to withstand 10,000 cycles of the

UTS of the native AF tissue. The testing setup was in reference to previous fatigue testing of Green et. al.[101] Testing was conducted on a Bose ElectroForce 3200 series, model: 3220, WinTest 7 (software), with a 100 lb. load cell. Representative samples were preheated to 37°C in a water bath for 30 minutes prior to testing and sample length, width, and thickness were determined using digital calipers. The samples were then attached by two U-shaped clamps with fine-grit sandpaper to prevent slippage of the material. The clamps were submerged in a bath chamber filled with sterile PBS solution and protease inhibitor. Once the samples were in place, the sample was aligned and brought taught to have a minimum of 0.5 N load on the tissue prior to testing. Once the sample was secured, preconditioning (5 cycles at 10% strain of the gauge length) was performed. Following preconditioning, the base plate was adjusted to apply a minimum of 0.5 N load to the sample. Axial tensile force was then applied on the patch (tension applied with alternating angles of $\pm$ 30° oriented in the vertical axis; n=16) at a pre-determined load [N] based on the representative percentage of UTS. Testing frequency was set at 0.5 Hz, and samples were ran until structural failure, or completion of 10,000 cycles. One cycle consisted of raising to the predetermined testing load with sample in tension, and lowering back down to the original testing load. The displacement, load control value, total time, cycles performed, and where the sample broke were recorded for statistical data analysis.

STATISTICAL ANALYSIS

Statistical analysis of the data were performed using Microsoft Excel or statistical analysis software (SAS Enterprise Edition 3.4, Version 9.4 or above). Results are represented as mean $\pm$ standard error of the mean Data was analyzed using a one-way ANOVA or by a two-tailed Student's t-test of unequal variance with significance defined as ($p < 0.05$).

CHAPTER III

RESULTS

PERICARDIUM SHEET FIBER ALIGNMENT AND AF PATCH ASSEMBLY

Our group has previously confirmed the decellularization of porcine pericardium via immunohistochemistry, agarose gel electrophoresis and Nanodrop analysis demonstrating the complete removal of alpha-Gal (porcine antigenic epitope), and a 95.3% decrease in DNA as compared to the fresh porcine pericardium, respectively.[147] This decellularization method was utilized before construction of AF patches.

Macroscopically, parietal pericardium sheets demonstrated a fiber preferred direction that was evident when the tissue was placed over a light box (**Figure 7A**). Histology of individual decellularized pericardium sheets confirmed the composition of the tissue (**Figure 8A**-**B**): dense regular collagen connective tissue (dense collagen type I fibers bundled and aligned in a parallel orientation, *left)* fused with dense irregular collagen connective tissue (dense arrangement of thick collagen type I fibers embedded in an amorphous ground substance, *right).* The average thickness of single-ply sheets of decellularized pericardium was 0.026 ± 0.002 mm.

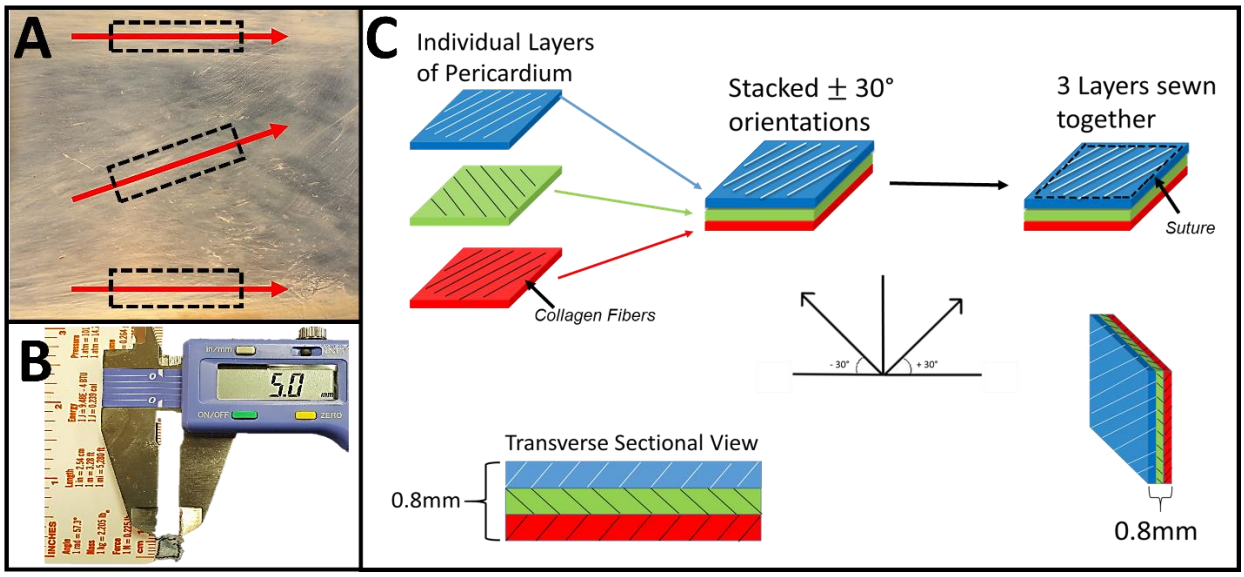

Figure 7: Fabrication of the AF patch through the alternation of individual sheets with collagen fibers oriented at ± 30° to a common horizontal axis. A) Representative image of a single piece of porcine pericardium. Arrows indicate collagen fiber preferred direction within each pericardium layer, and boxes (dotted outline) represent regions cut out for use in AF patches. B) Representative image of a 3-layer AF patch (5 [L] x 5 [W] x 0.8 [T] mm) following patch fabrication methods. C) Schematic representation depicting the fiber alignment in individual decellularized porcine pericardium sheets, subsequent stacking, and suturing of sheets together.

Multi-laminate patches comprised of 2, 3, 4, and 6 layers were successfully assembled having an average thickness of 0.05 ± 0.004 mm, 0.08 ± 0.006 mm, 0.11 mm ± 0.009 mm, and 0.16 ± 0.02 mm, respectively. The average length and width of multi-laminate patches for mechanical testing and cellular studies were 12 x 12 mm and 7 x 7 mm, respectively. Predetermined by testing protocols, different patch dimensions were constructed to fit into different test apparati. Patch sizes ranging from 4 x 4 mm to 30 x 30

mm were produced using our assembly method. Patches were assembled to mimic the human AF architecture with the multi-laminate sheets of porcine parietal pericardium aligned sequentially in alternating ± 30° to a common horizontal axis using a light box and secured by suture (**Figure 7C**).

CONFIRMATION OF ANGLE-PLY ARCHITECTURE

Composition and microstructure of the AF dictate its mechanical function. Based on the organization of collagen fibers between subsequent lamellae dictates the amount of intradiscal pressure the AF is capable of resisting. Therefore, to develop a biomimetic biomaterial mimicking the native AF, the resulting AF patch must be capable of presenting fiber alignment similar to the native tissue. To evaluate the capability of aligning porcine pericardium in alternating fiber alignment, polarized light microscopy and histology was used to confirm the orientation of the fiber preferred direction within each layer of the multi-laminate AF patches. **Figure 8C** illustrates the proof of concept demonstrating the successful construction of a 3-layered angle-ply patch with aligned collagen fibers orientations with the collagen fiber preferred direction running parallel to the viewer. While the proof of concept demonstrating the alternations of individual layers was demonstrated with the middle layer collagen fibers running parallel to the viewer, and the outer layer(s) collagen fibers aligned coming towards the viewer. (**Figure 8D)**.

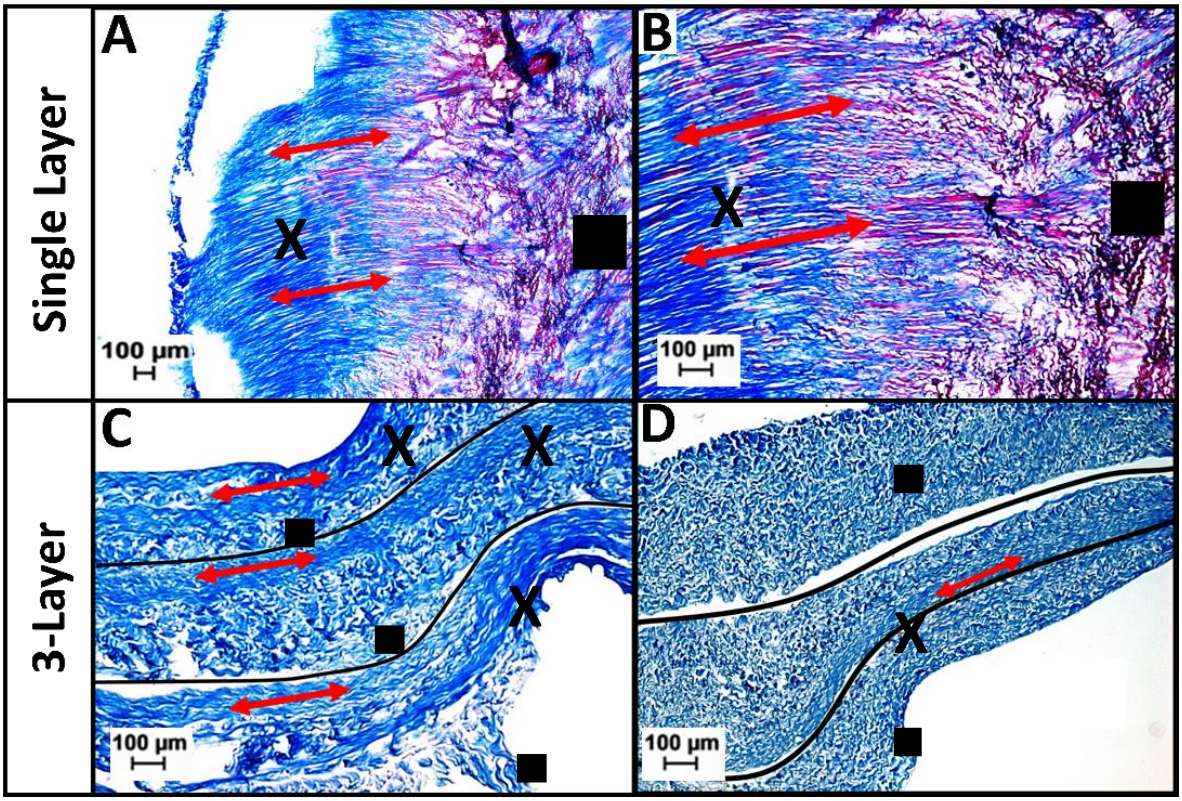

Figure 8: Histological analysis of decellularized porcine pericardium stained with Masson's trichrome (blue = collagen, red = cytoplasm), (arrow = fiber direction). A&B) Representative single layer pericardium illustrating dense regular connective tissue (X) and dense irregular connective tissue regions (■), (magnification: 100X and 200X, respectively). C&D) Histological image depicting the ability to alternate the fiber preferred orientation in additional pericardium sheets. Decellularized pericardial sheets were aligned based on alternating the angle of the fiber-preferred direction between each sequential layer (arrows indicate collagen fiber preferred direction within each pericardium layer), (magnification: 100X). [C] All three layers orientated with the collagen fiber preferred direction running parallel to the viewer, while [D] illustrates the alternation of fiber preferred direction with the middle layer

collagen fibers running parallel to the viewer, and the outer layer(s) collagen fibers aligned coming towards the viewer.

ULTIMATE TENSILE STRENGTH

To determine the ultimate tensile strength (UTS) and elastic modulus (EM) of the AF patch and to understand how fiber alignment impacts these properties, static tensile testing was performed on 3-layered multi-laminate AF patches, as well as, single layer sheets of pericardium. Single layer pericardium was tested in the fiber preferred (tensile load applied parallel to collagen fiber) and cross-fiber (tensile load applied perpendicular to collagen fiber) directions. Average UTS of a 3-layer AF patch, single layer fiber preferred, and single layer cross-fiber testing were 5.9 ± 0.3 MPa, 5.6 ± 1.1 MPa, and 2.9 ± 0.2 MPa, respectively (**Figure 9)**. A statistical difference ($p < 0.05$) was found between the UTS of three layered patches and single layer tissue oriented in the cross-fiber direction.

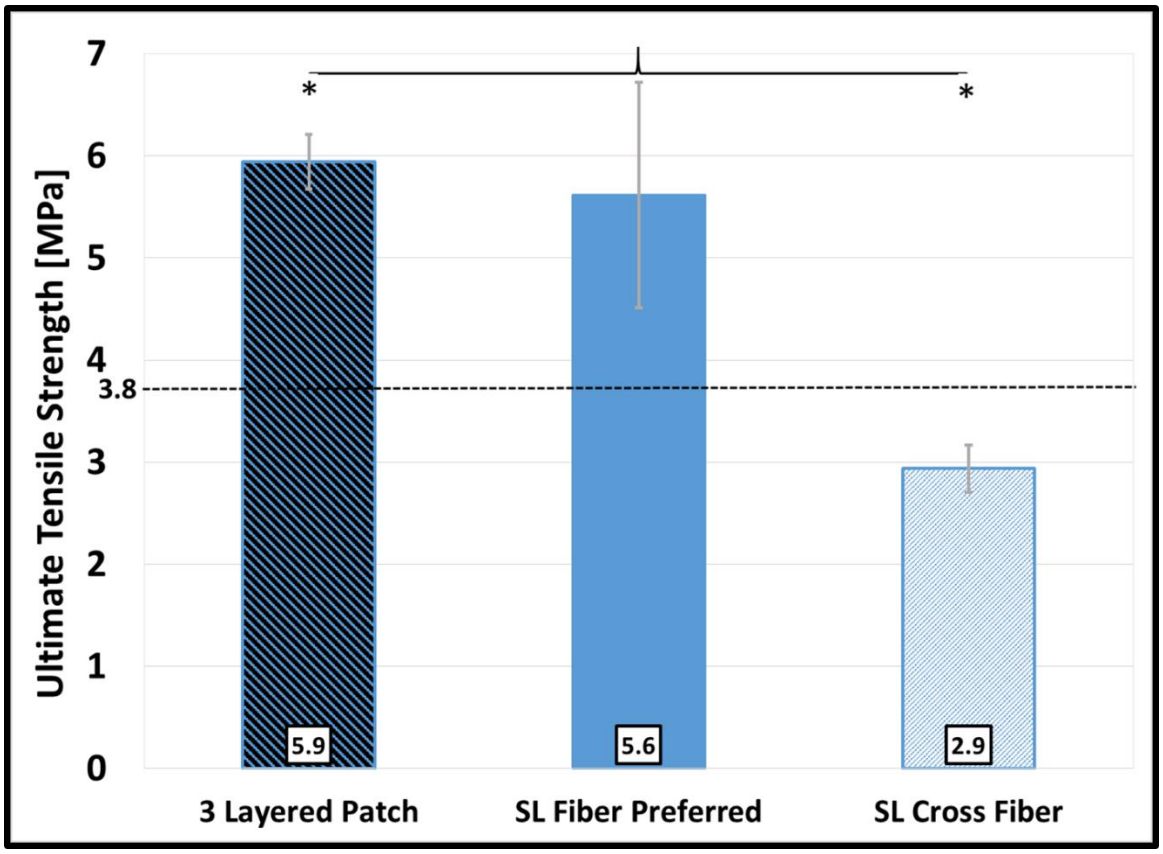

Figure 9: Tensile UTS of decellularized single layer sheets and 3-layered AF patches were tested, and values were compared to human AF (Dotted horizontal line indicates measured human AF UTS reported in literature).[101] The representative graph illustrates the average UTS for a 3 layered AF patch and single layer sheets aligned in fiber preferred and cross fiber directions. * indicates significant difference ($p < 0.05$).

EM was calculated from the linear region of the stress vs. strain graphs. Average EM of a 3-layer AF patch, single layer fiber preferred, and single layer cross fiber were 16.4 ± 3.5 MPa, 62.0 ± 13.6 MPa, and 23.6 ± 6.0 MPa, respectively (**Figure 10**). A

statistical difference ($p < 0.05$) was found between the EM of 3-layered patches and single layer tissue oriented in the fiber preferred direction.

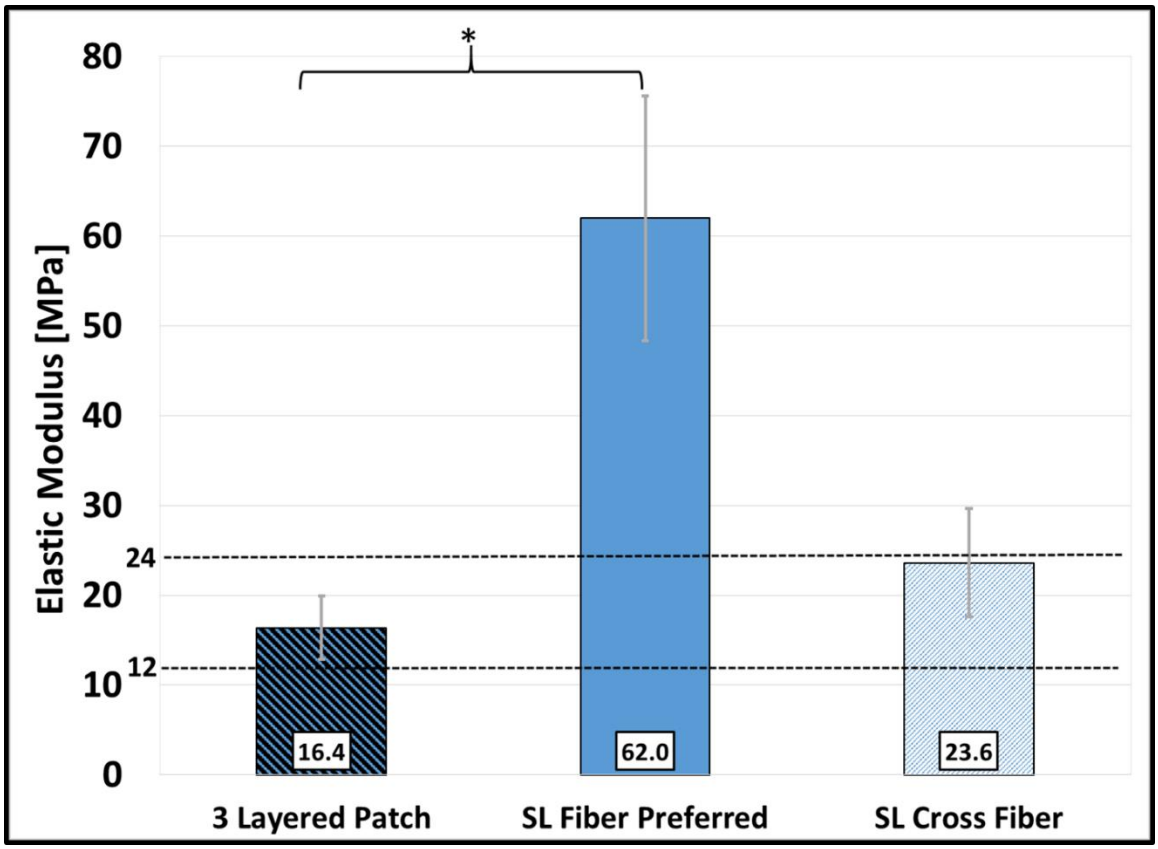

Figure 10: Tensile EM of decellularized single layer sheets and 3-layered AF patches were tested, and values were compared to human AF lamellae (Dotted horizontal line indicates measured human AF tensile modulus range reported in literature).[102] The representative graph illustrates the average tensile EM calculated from the linear region of the graph for decellularized 3 layered patch and single layer sheets aligned in fiber preferred and cross fiber directions. * indicates significant difference ($p < 0.05$).

AF PATCH RESISTANCE TO INSTANTANEOUS CHANGES OF INTRADISCAL PRESSURE

One of the primary mechanical functions of the AF is to resist the IDP generated by the NP. The IDP can change (increase) abruptly due to daily activities causing NP to herniate from native AF. Thus the ability of the AF patch to resist bursting open from a sudden increase in impact force/pressure was evaluated. The mechanical evaluation of instantaneous change of IDP for 1-layer, 2-layer, 3-layer, and 6-layer multi-laminar patches demonstrated an average impact resistance of < 6.81 MPa, 6.8 ± 0.0 MPa, 7.99 ± 0.22 MPa, and 9.94 ± 0.98 MPa, respectively (**Figure 11**). Single layer pericardium sheet impact resistance occurred at < 6.81 MPa, the lowest measureable amount of the custom designed testing apparatus. A linear increase in average impact pressure was observed with increasing layers included in the patch. Statistical difference ($p < 0.05$) was observed between 2-layer and 6-layer patches, and between 3-layer and 6-layer patches.

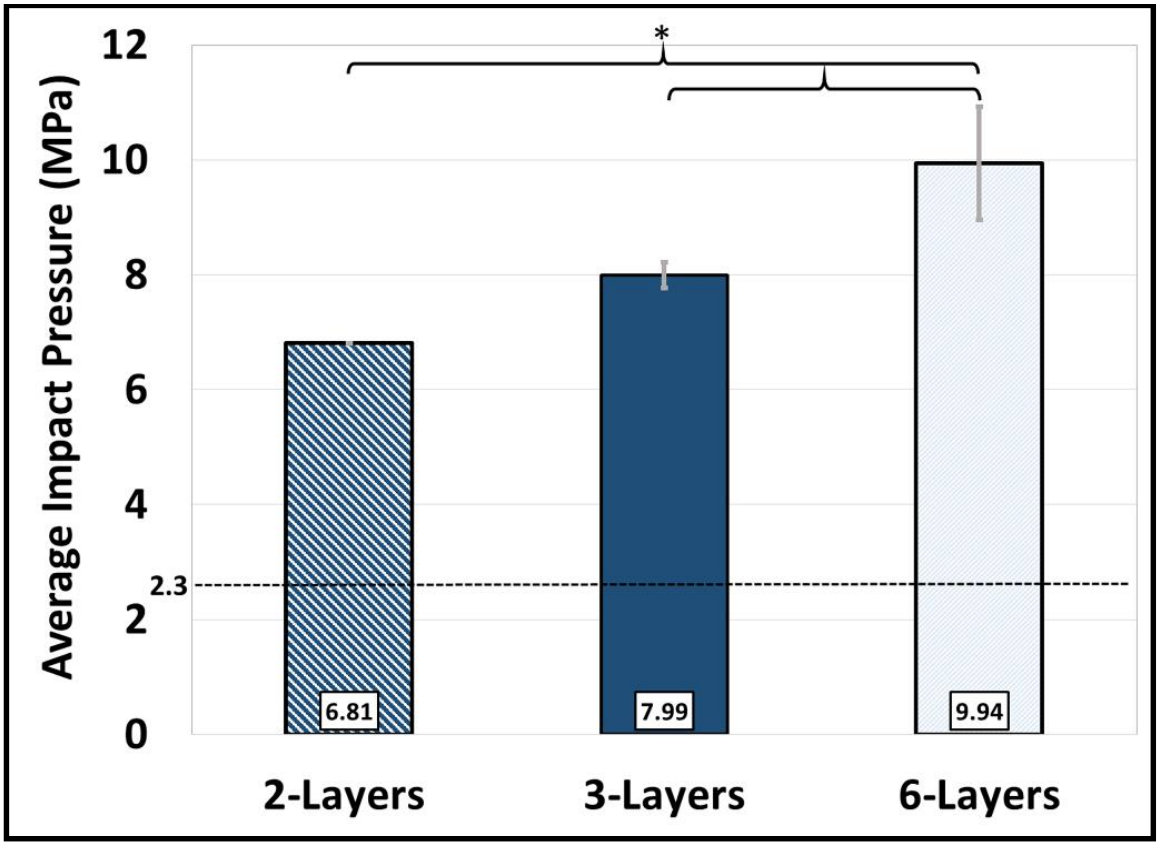

Figure 11: Impact resistance testing indicates multi-laminate AF patches can withstand instantaneous application of intradiscal pressure commonly experienced in the IVD. Representative graph of the average maximum calculated impact pressure withstood by a 2-, 3-, and 6-layer patches. (Dotted horizontal line indicates highest measured *in vivo* human IDP reported in literature [2.3 MPa observed while bent over with a round back while lifting 20 kg.]) * indicates significant difference ($p < 0.05$).

Previous testing conducted in our lab was conducted to determine the quasi-static burst strength of AF multi-laminate patches.[147] The burst strength testing protocol was adapted

from the ASTM D3786/D3786M: Bursting Strength of Textile Fabrics Method. The mechanical evaluation of the burst strength was performed for 1-layer, 2-layer, 3-layer, and 6-layer multi-laminar patches demonstrated an average impact resistance of at 4.26 ± 0.40 MPa, 7.53 ± 0.52 MPa, 10.75 ± 1.47 MPa, and 18.49 ± 0.76 MPa for, respectively (**Figure 12**).[147] Statistical difference ($p < 0.05$) was observed between all testing groups.

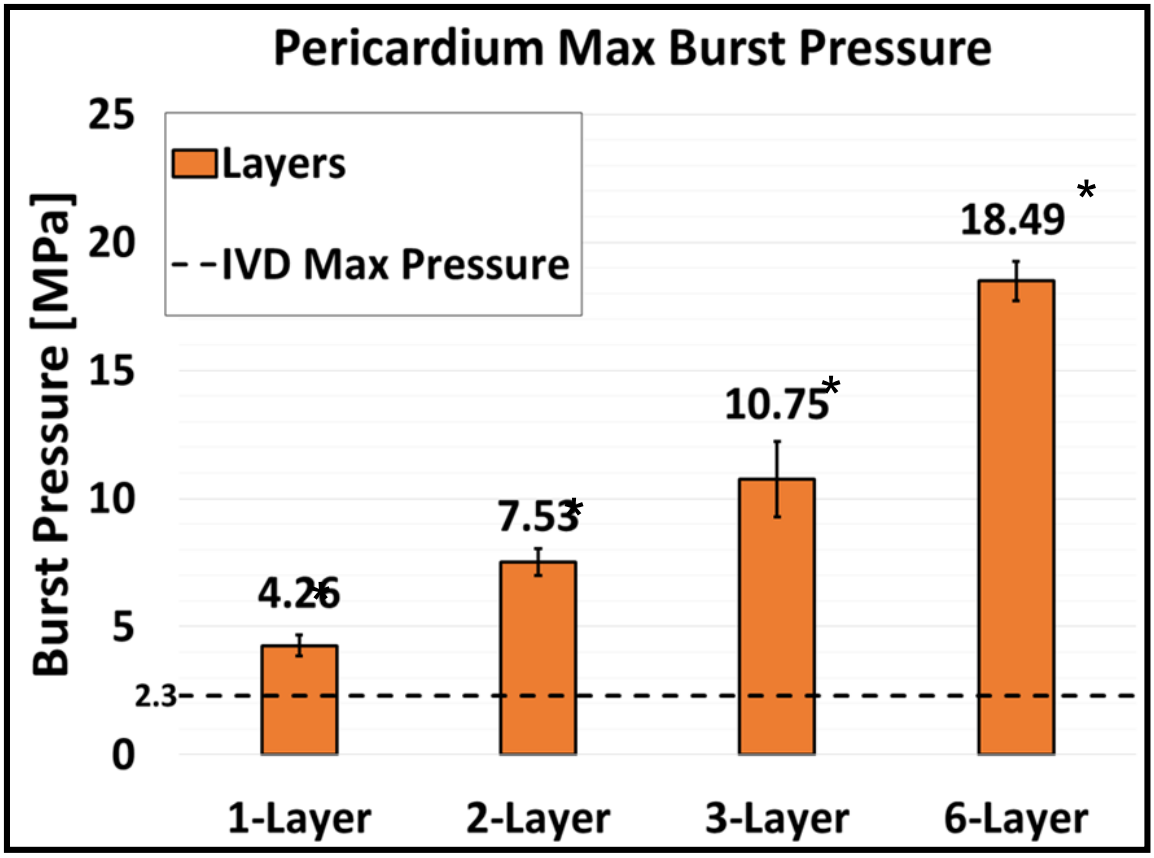

Figure 12: Burst resistance testing indicates multi-laminate AF patches can withstand quasi-static application of pressure commonly experienced in the IVD. Representative graph of the average maximum calculated burst pressure for 1-, 2-, 3-, and 6-layer patches. (Dotted horizontal line indicates highest measured *in vivo* human IDP reported in literature [2.3 MPa observed while bent over with a round back while lifting 20 kg.]) * indicates significant difference ($p < 0.05$). Picture reproduced with permission of R. McGuire.[147]

DYNAMIC TENSILE FATIGUE TESTING

One of the two primary spinal motions in the lumbar region is flexion. The bending motion associated with flexion is resisted by the posterior annulus and posterior longitudinal ligament. The ability of the AF patch to resist varying stress amplitudes during tensile fatigue loading was evaluated. Dynamic tensile fatigue testing of 3-layered multi-laminate AF patches was performed to predict the relative lifespan/endurance of the patch. Representative samples were tested to a mechanical run out of 10,000 cycles over a range of stress amplitudes observed during flexion to develop an S-N curve. Testing was conducted at stress amplitudes ranging between 0.95-2.66 MPa (25-70% UTS of the native human AF). AF patches withstood at minimum 1155 ± 75 cycles and achieved an endurance limit of 10,000 cycles at stress amplitudes of 2.66 MPa and 0.95 MPa, respectively. The S-N curve (**Figure 13)** illustrates the recorded data for AF patch overlaid on values reported for human AF tested under the same conditions. Supplemental data of Detailed applied load and cycles to failure of cyclic tensile fatigue experiments are listed in (**TABLE 6**).

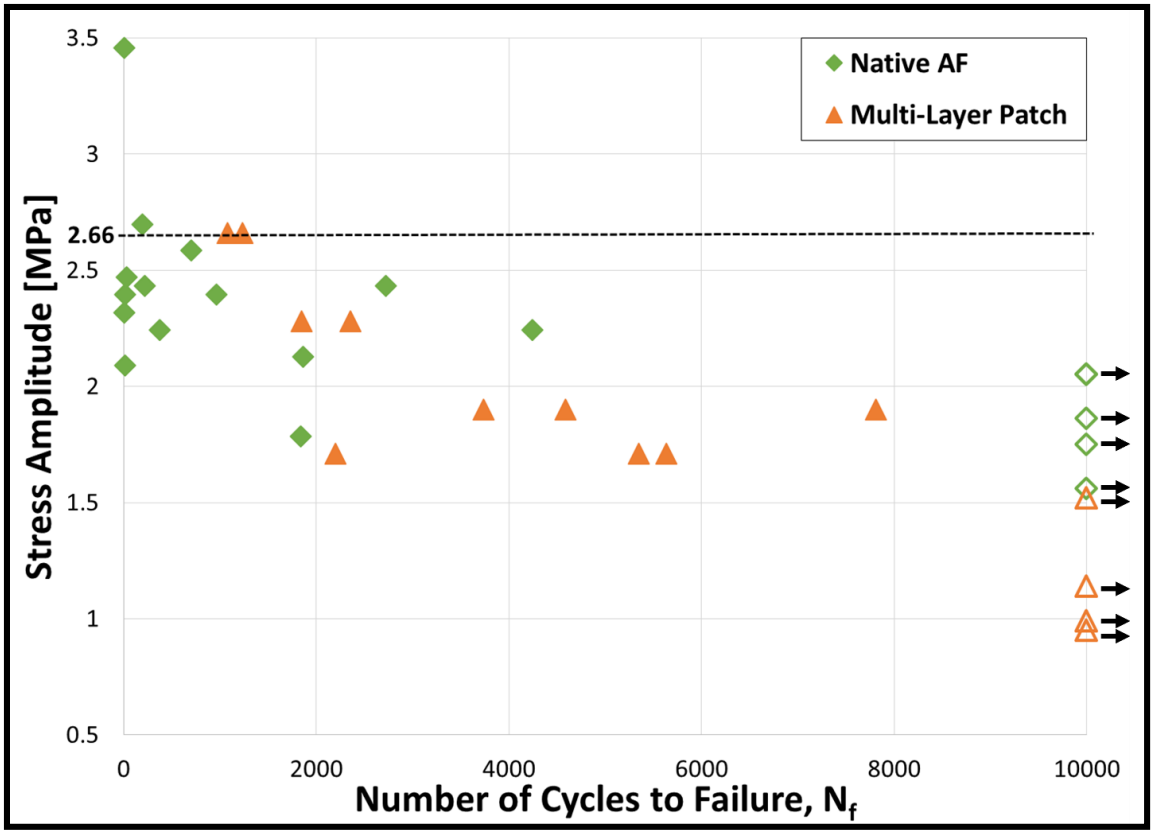

Figure 13: Tensile fatigue endurance of 3-layer AF patch approximates that of the native human AF. S-N Curve illustrating the fatigue strength of our 3-layered multi-laminate AF patch (triangles), in comparison of native human AF (diamonds).[101] A negative correlation between the level of applied stress and the number of loading cycles to failure was observed. Open diamonds, triangles, and arrows indicate specimens with no mechanical failure observed (mechanical run out to 10,000 cycles).

Table 6: Detailed applied load and cycles to failure of cyclic tensile fatigue experiments with native AF (left) vs. 3-layered multi-laminate AF patch (right) based on representative UTS (Ultimate Tensile Strength) percentages. Tests were halted following a mechanical run out to 10,000 cycles.

Loading Details

Native AF[7]			Multi-layered AF Patch		
Load (% UTS)	Load (MPa)	Cycles to failure	Load (% UTS)	Load (MPa)	Cycles to failure
41	1.56	10000	50	1.90	3740
46	1.75	10000	50	1.90	7810
47	1.79	1835	50	1.90	4590
49	1.86	10000	45	1.71	2200
54	2.05	10000	45	1.71	5630
54	2.05	10000	45	1.71	5350
55	2.09	14	25	0.95	10000
56	2.13	1860	26	0.99	10000
59	2.24	371	60	2.28	2350
59	2.24	4245	30	1.14	10000
61	2.32	5	40	1.52	10000
63	2.39	15	60	2.28	1850
63	2.39	960	70	2.66	1230
64	2.43	215	70	2.66	1080
64	2.43	2720			
65	2.47	27			
68	2.58	700			
71	2.70	195			
91	3.46	5			

CELLULAR ANALYSIS

Cellular studies were conducted on 3-layered multi-laminate angle-ply AF patches to ensure cell viability on all layers of the patch. Previous laboratory testing showed that bovine AFCs were viable on the surfaces of the patches through day 15 studies;[147] however, following histological analysis cell viability between the upper and lower layers were previously unidentifiable. To provide the greatest chance of probability of cell attachment,

a volume optimization protocol was used to determine the total amount of volume (µl of cell culture media containing AF cells) an AF patch was capable of holding to prevent run-off. It was determined a 7 x 7 x 0.8 mm^3 AF patch was capable of holding 45 µl on the top and bottom layers, and 75 µl between the layers before run-off occurred.

Tissue disruption modification (sonication) was used with the hypothesis of disrupting the tissue extracellular matrix to provide more nutrient transfer to the inner layers. Histological analysis of representative control and sonicated 3-layered multi-laminate AF patches of days 3 and 6, respectively, illustrated cell attachment and infiltration (**Figure 14**). Histological evaluation illustrates AF cell attachment on all layers of the multi-laminate AF patch for all samples and time points investigated.

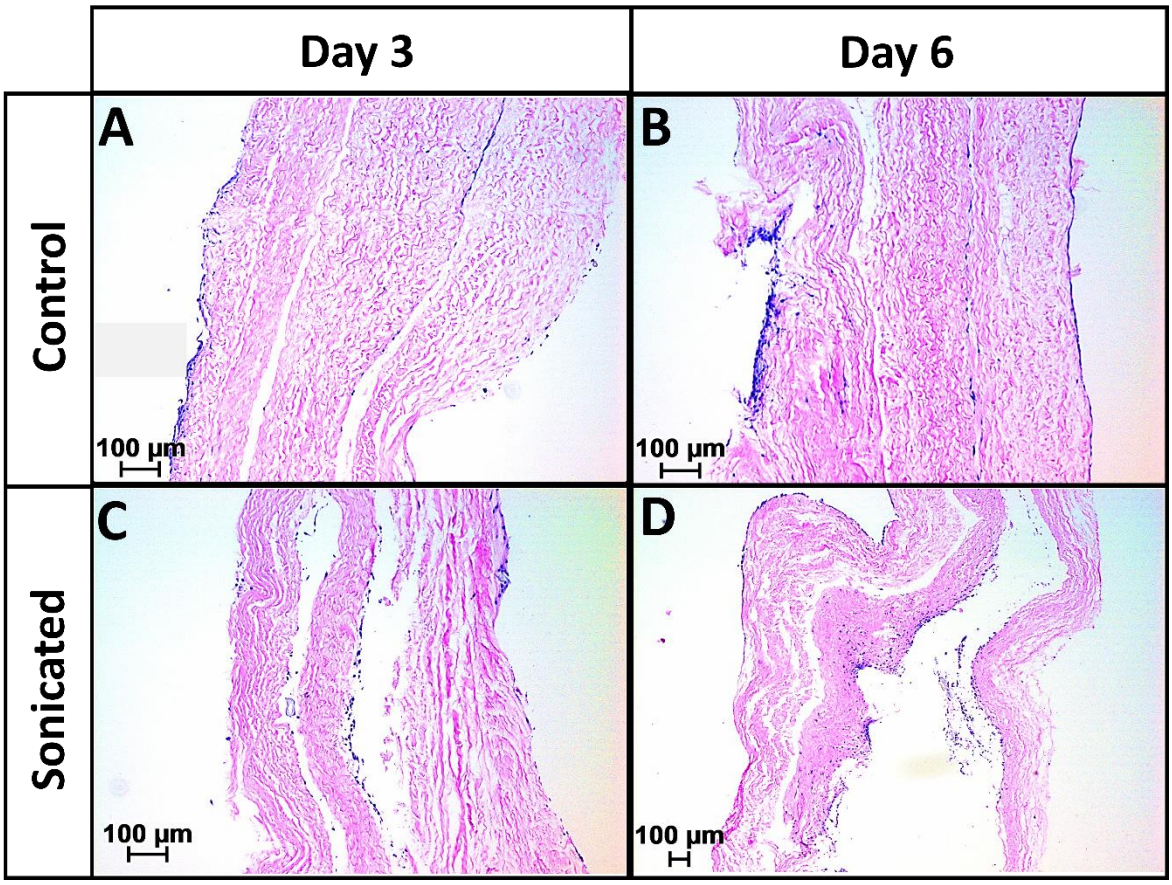

Figure 14: Multi-laminate AF patches support AF cell viability, and infiltration demonstrated through stained H&E (purple = cellular nuclei, pink = ECM) samples. A-B) Representative histological cross-sectional images depicting the presence of AF cells within the tissue of a 3–layer multi-laminate AF patch at days 3 and 6 stained with H&E (magnification: 100X). C-D) Representative cross-sectional histological images depicting the presence of AF cells within the tissue of a 3–layer multi-laminate sonicated AF patch at days 3 and 6 stained with H&E (magnification: 200X and 50X, respectively).

Representative sections of day 6 AF patches for sonicated and controlled tissues were magnified to perceive clearly the cells infiltrated into the tissue (**Figure 15**). The

width of the representative tissue layers were measured and recorded at 538 µm and 483 µm (**Table 7**). Average measured cell penetration depths for sonicated and control sample AF patches, measured using ImageJ software, were 278 µm and 52 µm, respectively. The furthest depth of cell infiltration were 503 µm (93.7% overall depth relative to tissue width) and 327 µm (67.7% overall depth relative to tissue width). A statistical difference ($p < 0.05$) was observed between the average cell infiltrations of sonicated and control patches on day 6.

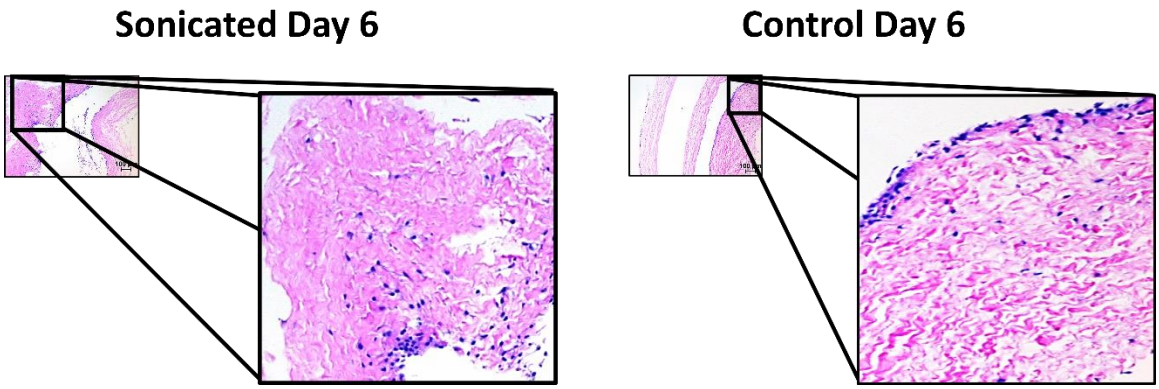

Figure 15: Increased magnification of a multi-laminate AF patch section, one of the three layers, depicting infiltration of cells into the tissue layers for day 6 sonicated and controlled AF patches. (*Left*) Sonicated tissue treated for 20 minutes at time point day 6. (*Right*) Control tissue at time point day 6. (Left and Right original magnification: 200X).

Table 7: Measurement and analysis were conducted to illustrate cell infiltration. To determine the depth of penetration by the AF cells H&E histological staining and ImageJ software were used. Representative sections of a 3-layered multi-laminate AF patch were magnified (Figure 9) to perceive clearly the cells for sonicated and control tissue samples. Width of the representative tissue layers were measured, and average/deepest depth of cell infiltration was analyzed for sonicated and control tissue samples, respectively. For average and deepest cell infiltration, the percentage of overall depth relative to tissue width is displayed in parenthesis. * indicates significant difference ($p < 0.05$).

Day 6 (AF Patch) Cell Infiltration Measurement

	Sonicated	Control
Width of Layer	538 µm	483 µm
Average Cell Infiltration*	278 µm (51.7%)	52 µm (10.7%)
Deepest Cell Infiltration	503 µm (93.5%)	327 µm (67.7%)

CHAPTER IV

DISCUSSION

Effective biological AF repair is an unmet clinical need for several applications: to prevent recurrent IVDHs, to preserve the IVD biological structure and functionality, and/or to support NP arthroplasty devices for patients with early stage interventions targeting IVDD. An ideal AF repair device must mimic the biological, structural, and functional characteristics while promoting tissue regeneration. The native AF is comprised of highly organized lamellae of aligned type I collagen fibers. When entirely intact, the AF confines the NP to the center of the IVD and provides resistance to IDP generated by the NP. When a defect is present, the associated underlying pathology and surgical repair typically contribute to long-term pain and long-term effects on adjacent IVDs (adjacent segment degeneration).

Until recently, clinicians believed pain associated with IVDH would resolve on its own without surgical intervention (i.e. spontaneous resorption of the herniation). However, despite a temporary reduction in pain, a recent study indicated when herniations were left untreated, a resurgence of pain occurs.[50] For patients presenting with radicular symptoms or low back pain that is unresponsive to conservative therapy, and demonstrate through magnetic resonance imaging (MRI) or computed tomography (CT) confirmation of an NP herniation or extrusion, a discectomy procedure is often warranted.[148] Annually, there are over 500,000 lumbar discectomies performed in the United States.[50] While this procedure yields satisfactory clinical outcomes, an open pathway (defect) remains which provides a path of least resistance for recurrent IVDHs to manifest. It has been shown, the rate of re-

herniation is greater in patients with an AF defect larger than 6 mm.[10,149] The wide variety of approaches and techniques used to perform a discectomy can be debated with respect to their advantages and disadvantages. While a less aggressive discectomy approach (removing the protruding NP fragment without an extensive intradiscal compression) results in improved patient outcomes, it does present a greater risk for re-herniation as compared to an aggressive approach (removal of more than the protruding NP tissue [disc decompression] in attempts to decrease the likelihood that re-herniation may occur).[54] Therefore, an effective AF closure/repair device in conjunction with a less aggressive discectomy may result in improved patient outcomes, decreased pain, and fewer revision surgeries via lower re-herniation rates.[5,6] Additionally, with the application of an AF closure device, it could lead to a reduction of chemical pain mediators escaping through the open AF following a conventional discectomy, thus reducing the effects of irritation of the nerve root ganglion, epidural fibrosis, or the potential for ingrowth of nerve fibers that are mediators of postoperative discogenic pain.[150–152]

The discectomy procedure itself is not benign to the disc – it is an ablative, not a restorative procedure.[148] Suturing is a simple and appealing repair method to be used for AF closure due to its frequent use during surgery; however, suturing does not account for missing AF tissue and may not be strong enough to resist changes in intradiscal pressure (IDP).[5,6,16] Therefore, there has been an increase in tissue engineering and regenerative therapeutic being investigated over the last decade aiming to structurally and biologically repair the AF.

A need exists to develop an AF closure/repair device that mimic the architecture (multi-laminate lamellae of aligned collagen oriented in an angle-ply fashion), mechanical properties (ultimate tensile strength and modulus), cytocompatibility (ability to promote cell viability and regeneration), and function (ability to resist tensile loading, intradiscal pressures, and fatigue) of the native human AF. The objective herein was to confirm our ability to generate multi-laminate patches comprised of decellularized porcine pericardium with a repeatable angle-ply architecture, to mechanically evaluate their strength and durability, and assess their cytocompatibility. It is hypothesized that the AF patches composed of decellularized porcine pericardium would mimic the biological, structural, and functional characteristics of the native AF, and therefore, be an ideal surrogate for use in its repair.

PATCH FORMATION

The development of the biomimetic AF patch that mimics the native human AF architecture was vital. The alternation of collagen fibers between the native lamellae is the underlying foundation of what provides the AF strength when distributing the tensile bending and torsional forces throughout the functional spinal unit.[153] The parietal pericardium layer from porcine hearts was chosen due to its natural underlying structure. The parietal pericardium is fused to and inseparable from the fibrous pericardium (most superficial layer of the pericardium). It consists of dense and loose connective tissue comprised of collagen type I,[143] mimicking the native composition of the AF. The dense connective tissue is divided into regular and irregular sections. Dense regular connective

tissue contains collagen type I fibers bundled in a linear/parallel orientation. The presence of these collagen fibers was utilized during fabrication of the scaffold.

By manually alternating the fiber preferred direction of the dense regular fiber architecture of the decellularized porcine pericardium over a light box, a repeatable method to overlay consecutive sheets of pericardium achieving an angle-ply orientation was developed. Following the alignment of subsequent layers, the patches were secured together using suture. The simplicity of this technique combined with the need for different sized patch dimensions for testing protocols, patient IVD height, and varying patient AF defect sizes allowed for the construction of patches ranging in size from 4 x 4 mm to 30 x 30 mm using our assembly method. The mean disc height reported for the lumbar segment of the spine were 11.6 ± 1.8 mm for the L3/4 disc, 11.3 ± 2.1 mm for the L4/5, and 10.7 ± 2.1 mm for the L5/S1 level.[154] While not surprisingly, the size of an AF defect exhibits an enormous effect on the re-herniation rate. In patients with massive AF defects (> ~6-6.5 mm), the re-herniation rate was 27% compared to patients with slit defects who experienced re-herniation rates of only 1%.[10] Thus, based on these results, it would indicate that if larger defects are effectively reduced in size, re-herniation rates could fall dramatically in this "at-risk" group of patients.[148] Taken together, we were able to produce patch sizes that are of clinical utility. In addition, the development method employed to make these patches can be easily scalable for batch manufacturing procedures compared to other formation methods of AF scaffolds which require more complex manufacturing techniques.[155]

CONFIRMATION OF ANGLE-PLY ARCHITECTURE

Verifying the proof of concept creating an angle-ply AF patch architecture was demonstrated through histological images of single sheets and three layer stacking. Masson's trichrome staining and polarized light microscopy was used to view the fiber preferred direction histologically. Polarized light microscopy was used to refract the light based on collagen fiber orientation within the individual layer of pericardium. Since collagen fibers are an anisotropic material, it expresses birefringent under polarized light. With this optical property, the fiber preferred direction of the porcine pericardium were clearly visible to correspond to the fibers seen macroscopically. When stacked in multiple layers, the AF patch demonstrated the proof of concept for the alternation of fibers with the collagen fibers visible in the individual layers aligned coming towards the viewer, and the alternating layers oriented away from the viewer.

MECHANICAL TESTING OF AF PATCH

Of the available repair methods for AF regeneration, decellularization of an extracellular matrix derived scaffold is an attractive option due to its ability to promote the expression of M2 macrophages (immune cells with the ability to promote tissue homeostasis through cell proliferation and tissue repair)[156] and its ability to preserve the tissues microenvironment.[157] In addition, these attributes promote cell survival, proliferation, morphogenesis, differentiation, and constructive tissue remodeling.[158,159] However, the decellularization process of a biological tissue can have potentially significant effects on the biomechanical properties of the resulting scaffold. Thus, it is critical to evaluate how closely the mechanical characteristics of the resultant AF patch

compare to the values of the native human AF. Although the mechanical advantage of closing annular defects to retain NP material seems intuitive, only recently have AF closure devices been examined for their ability to withstand in situ IDP or flexibility testing.[16] For this reason, it was paramount to evaluate the mechanical characteristics of our multi-laminate angle-ply AF patches with respect to tensile strength, impact resistance, and tensile fatigue.

UTS TESTING

To characterize the maximum tensional stress our AF patch is capable of resisting, representative samples were placed under a static tensile load to develop a stress-strain relationship. These values were then compared to reported human AF tissue to approximate the maximum tensile loads endured by the AF during flexion/bending. The AF patch illustrated mechanical properties of UTS and elastic modulus (EM), which fell within the reported values of the native human AF (3.8 ± 1.9 MPa, and 12-24MPa, respectively).[101,102] The biological function of a collagen-based material lies predominantly in its mechanical properties. The viscoelastic biological tissue (combined with strong underlying cross-linking fibers)[160] expressed both viscous and elastic properties when undergoing deformation. This particular behavior results from the anisotropic microstructure of the AF tissue composed of oriented collagen fibers embedded in the ECM.

The measured UTS represents the maximum stress that the material could withstand before failing, and is correlated with the highest stress value on the stress-strain graph. Collagen fibers have the optical property of birefringence that defines the direction they

can bear a load in a tissue, and the strength of birefringence has been correlated with the UTS.[161] In a stress-strain relationship, the EM is calculated from the linear portion of the graph up to the yield point of the material. As a material stiffness increases it expresses a higher EM. The low EM of the AF patch demonstrates its flexibility and ability to change shape while maintaining a relatively high UTS similar to the native AF tissue.

The UTS and EM of the single layer fiber preferred direction were shown to be greater than the single layer cross-fiber direction. This is attributable to the mechanical function of the collagen fibers that work to resist tension, and while applying a load perpendicular to or at an angle from the primary axis of the fiber preferred direction would essentially cause the interstitial matrix to endure the majority of the stress, not the fibers themselves. The difference seen between the fiber preferred and cross-fiber directions is also consistent with acellular scaffolds and continuous fibers in composite materials consisting of predominantly collagen fibrils. These acellular scaffolds and continuous fibers demonstrated the mechanical properties of the fiber preferred orientation and resulted in higher tensile strength and stiffness (elastic modulus) compared to that of the cross-fiber preferred direction.[162,163]

Analysis of tissue behavior increases in complexity as the hierarchical tissue structures become more complicated. The AF patch (aligned with $\pm$ 30° alternations between subsequent layers) expressed higher UTS compared to single layer tissue aligned in the fiber preferred direction and cross-fiber direction. This is consistent with mechanical testing of angle-ply laminates which found that opposing ($\pm$ 30°) constructs were stronger than the fiber preferred aligned constructs.[132] While another study showed that during

uniaxial tensile loading on various fiber angles, the elastic moduli varied with a nonlinear decrease seen in modulus with increasing fiber angles.[120]

Even though axial rotation and lateral bending in the lumbar discs are relatively limited, the range of motion of the IVD in flexion-extension can be as high as 24 degrees.[164] Because the center of rotation of the disc is typically anterior of the posterior AF, the strain range of the posterior AF during these high ranges of motion can vary greatly. Maximal physiologic strains observed along the AF superficial tissue are about 4% when the disc is in compression or torsion, and ~6% when the disc is in flexion or extension, but never exceeding 10%.[165] Thus, designing a device that can maintain its integrity while sealing defects that also go through this strain range is extremely challenging.[148] The amount of strain experienced to reach the UTS of our AF patch, relative to the native AF tissue UTS, was 5.7 $\pm$ 0.43 mm. Thus demonstrating the ability of our AF patch to undergoing the native strain range, while maintaining its tensile strength integrity.

FATIGUE TESTING

To assess the capability of the AF patch withstanding dynamic loading, the AF patch underwent tensile fatigue testing for ranges of 25-70% UTS. Upon characterizing the UTS of the AF patch, it was necessary to address the levels of stress amplitude commonly experienced by the AF during flexion. The representative testing range, of 25-70%, was performed based on the lower range limit determined from the resulting endurance limit of the AF patch. While the upper range limit was chosen to be 70% (due to the fact, when placed *in vivo*, the IVD is unlikely subjected to stresses higher than 70% UTS due to the prevention of injury by ligaments of the neural arch during extension and lateral bending,

and through soft tissues during flexion).[166] Comparative analysis of the AF patch and native human AF, illustrated by **Figure 7,** demonstrates the AF patches display of a similar S-N curve profile relating the level of applied stress to the number of loading cycles withstood prior to failure.

Adapted from a previously published testing protocol for AF tensile fatigue testing,[101] 10,000 cycles were chosen for the mechanical run out of our AF patch. This was not to represent a true fatigue limit, but an estimation of how a biological tissue will last in a theoretical environment absent of intrinsic healing. While the AF is constantly subjected to cyclic tensile loading, typically the higher maximum tensile stresses only occurs during a limited range of motions, such as bending forward at the waist (without bending your knees), sitting down in a low chair, or tying your shoes. When damage to the AF does occur, the intrinsic healing process begins. The AF is identified to heal in three phases: 1st phase is when the outer AF begins to heal (day 0 – few weeks), 2nd phase is when the interior AF layers gradually heal (few weeks – one-year), and 3rd phase is when there is an increase of collagenous fibers within the NP.[112] Based on the tensile fatigue results, the AF patch has the capability to resist failure for between 1.0-2.7 years (conservatively assuming achievement of maximal flexion approximately 10-25 times per day), which is beyond the reported time required for native AF healing (which would eventually help off-load the mechanical patch responsibilities).[112] Therefore, it is reasonable to assume that when placed under tensile loading the AF patch is capable of meeting the mechanical demands experienced during flexion for the posterolateral AF.

IMPACT TESTING

Impact mechanical testing was performed to obtain the minimum number of layers required to withstand the changes of IDP generated by the NP of an IVD. Currently, IDP measurement is the only direct way to determine the loading conditions within the human spine.[48] The posterior region of the AF is inherently weaker due to its more parallel alignment to the horizontal axis of the spine compared to other regions.[29] Combined with instantaneous changes of IDP within preceding IVDH defects and/or discectomy procedure sites provide a weakened region in the AF lamellae that have been linked to the rupture of the AF; therefore, it was crucial to characterize the impact resistance for the AF patch.[167] The AF patch must be capable of enduring the maximum impact force generated by the NP since the vacant area beneath the patch will represent the entire thickness of the AF in the repaired region.

Previously reported by our group, the quasi-static burst strength of the AF patch was calculated to determine the approximate amount of layers required to withstand typical IDP values generated by the NP.[147] While herniations typically occur from a gradual degeneration of the disc (weakening of the posterior AF), the rate of IDP change varies based on AF tissue degradation and movement of the patient. Currently, no published studies specify the speed at which a herniation occurs in nondegenerated IVDs. Using calculations based on the reported IDP ranges seen in the native human AF, (0.1-2.3 MPa),[167–169] combined with the idea that an instant change of force can lead to an increase in stress concentrations, the AF patches were tested at varying forces with a constant velocity of 2.23 m/sec. This velocity is consistent with compression testing conducted to

measure the failure mechanisms of the impact loading on the spine,[170,171] and represent greater speeds than are commonly tested for physiological responses to impact loading.[172–174] The impact resistance measured of AF patches indicated its ability to withstand instantaneous changes of IDP observed within the human IVD. A linear increase in average impact resistance was observed with increasing the number of pericardium layers within the AF patch. While theoretically, the amount of layers required to withstand instantaneous changes in IDP commonly observed was less than three layers (optimized value chosen for the AF patch), previous results from the quasi-static burst strength testing illustrated a need for the minimum of 3-layers. Additionally, this impact mechanical testing does not account for repetitive cyclic increases in IDP which would be seen *in vivo*. Future studies will be conducted to measure the efficacy of the patch to resist cyclic IDP and containment of the NP material through dynamic compression fatigue resistance testing, following attachment to cadaveric IVDs.

CYTOCOMPATIBILITY OF CELL SEEDING ON AF PATCH

Aside from the AF patch having mechanical characteristics that closely approximate the human AF, it is also made of a biologic material that may lead to the promotion of tissue regeneration. This is something that cannot be said about synthetic AF repair techniques/materials. The regenerative potential the biological AF patch possesses is an advantage in the way it will aid in self-repair and integration. Following attachment of the AF patch to the native IVD, the entire mechanical load is supported by the biomaterial scaffold and attachment mechanisms. Thus, the patch must maintain sufficient mechanical strength to support physiological loading. With the potential increase of

integration between the AF patch and native AF tissue over time, the applied loads on the patch will decrease; thus, assisting in the durability of the AF patch and attachment mechanism. It is reported that AF regeneration could potentially be enhanced by the supplementation of cells to accelerate the healing process of large annular defects.[130] While this is not essential as a mechanical surrogate, the AF patch should be capable of, at the minimum, supporting cell viability of cells within the patch as well as potentially promote the migration of neighboring cells into the patch.

Tissue engineering scaffolds are developed to influence the physical, chemical, and biological environment surrounding a cell population.[175] The use of cells affects the scaffolds ability to regenerate the ECM by maintaining the long-term homeostatic balance of matrix turnover.[176] Therefore, cytocompatibility studies were conducted to evaluate the AF patch ability to allow for cell infiltration of viable AF cells. Bovine AF cells were used in the current study to test for cytocompatibility of the AF patch with cells representing an end-stage phenotype found in the native AF. While bovine AF cells were suitable for studying the effects of cell behavior on the AF patch, there is a need for an alternative cell source if it is to be used in a clinical setting. Allogenic AF cell isolation requires the patient to be subjected to an invasive surgical procedure, and xenogeneic AF cells are not a viable option. Therefore, the use of stem cells integrated within the AF patch during implantation needs to be investigated to identify potential improvement for regeneration capabilities of the patch. This will be addressed in future studies.

The previous testing conducted in our lab demonstrated the viability of AF cells on the outer layers of the AF patch; however, histologically cells were not observed within

the inner layers.[147] It was assumed that the cells seeded on the inner layers may have undergone premature cell death and detached before histological analysis was conducted due to the dense ECM preventing the nutrient transfer. However, the current study presumed that a non-optimized cell seeding process could have contributed to the failure of cells attaching to the inner layers. Therefore, a cell suspension volume optimization protocol was developed to ensure cell seeding accuracy. Additionally, ultrasonication studies were conducted with the intent of disrupting the ECM of the AF patch layers in order to improve nutrient transfer and cell migration within the inner layers of the AF patch.

The results indicated the AF patch does allow for the attachment and infiltration of AF cells in all three layers for an extended period, and is capable of supporting cell viability. This was true for both the control (non-sonicated) samples and sonicated samples. While the volume optimization protocol ensured cell attachment on the inner layers of the AF patch was feasible without tissue disruption, sonicated samples showed a statistical difference in the distance cells were capable of infiltrating into the tissue; however, sonication treatment of the AF patches could also potentially weaken mechanical properties.

CHAPTER V

CONCLUSIONS & RECOMMENDATIONS FOR FUTURE STUDIES

Coupled with our previously reported findings that illustrate the simplicity and scalability of our patch formation method concurrent with its ability to support AF cell attachment, these mechanical testing data suggest our AF patch is an ideal surrogate to replace and regenerate the native human AF tissue. Overall results show similar mechanical properties to native human AF tissue through the ultimate tensile strength and elastic moduli, the ability to resist instantaneous changes of IDP, and strength to withstand tensile fatigue mimicking the intact (15-25 layer) native human AF. Thus, our device could improve patient outcomes and lower healthcare costs for those with IVDH by allowing for the utilization of less aggressive discectomy, minimizing the reoccurrence of IVDH, and may allow the use of early-stage interventions including nucleus arthroplasty for those with IVDD. Future studies should include burst fatigue strength, animal studies, and further cellular characterization studies (stem cell seeding, GAG content, and cross-linking between the layers).

REFERENCES

1. Herper M. Making Back Surgery Obsolete. 2010. http://www.forbes.com/2010/06/11/back-surgery-medtronic-healthcare-business-j-and-j-spine.html.

2. Praemer, A. Furner, S. Rice D. Musculoskeletal Conditions in the United States. *Am Acad Orthop Surg*. 1999.

3. Sharifi S, Bulstra SK, Grijpma DW, Kuijer R. Treatment of the degenerated intervertebral disc; closure, repair and regeneration of the annulus fibrosus. *J Tissue Eng Regen Med*. 2014;(FEBRUARY). doi:10.1002/term.1866.

4. Martin B et al. Expenditures and health status among adults with back and neck problems. *JAMA*. 2008;299:656-664.

5. Bailey A, Araghi A, Blumenthal S, Huffmon G V. Prospective, multicenter, randomized, controlled study of anular repair in lumbar discectomy: two-year follow-up. *Spine (Phila Pa 1976)*. 2013;38(14):1161-1169. doi:10.1097/BRS.0b013e31828b2e2f.

6. Lequin MB, Barth M, Thom C, Bouma GJ. Primary Limited Lumbar Discectomy with an Annulus Closure Device : One-Year Clinical and Radiographic Results from a Prospective , Multi-Center Study. 2012;9(4):340-347.

7. Nerurkar NL, Baker BM, Sen S, Wible EE, Elliott DM, Mauck RL. Nanofibrous biologic laminates replicate the form and function of the annulus fibrosus. *Nat Mater*. 2009;8(12):986-992. doi:10.1038/nmat2558.

8. Bajanes, G. Perez, A. Dias M. One year follow up of discectomy patients who received a mesh to repair the annulus fibrosus. *Spine Arthroplast Socitey*. 2006;7.

9. Bourgeault, C. Beaubien, B. Griffithy S. Biomechanical assessment of annulus fibrosus repair with suture tethered anchors. *Spine Arthroplast Socitey*. 2007.

10. Carragee EJ, Han MY, Suen PW, Kim D. Clinical outcomes after lumbar

discectomy for sciatica: the effects of fragment type and anular competence. *J Bone Joint Surg Am*. 2003;85-A(1):102-108.

11. Cauthen J. Microsurgical reconstruction (annuloplasty) following lumbar discectomy: preliminary report of a new technique. *Proc AANS/CNS Jt Sect spine Peripher nerves, Orlando*. 1999.

12. Gorensek, M. Vilandecic MW. Clinical investigation of intrinsic therapeutics Barricaid, a novel device for closing defects in the annulus. *NASS*. 2007.

13. Kamaric, E. Gorensek, S. Trummer M. Surgical factors affecting after lumbar discectomy: the need for an anular closure device. *In Thera*. 2007.

14. Sherman, J. Cauthen, J. Griffith S. Pre-clinical evaluation of a mesh device for repairing the annulus fibrosus. *Spine Arthroplast Socitey, Berlin*. 2007.

15. Taylor W. Biologic collagen PMMA injection (artifill) repairs mid-annular concentric defects in the ovine model. *Spine J*. 2006;6(5S1):48S - 49S.

16. Bartlett A, Wales L, Houfburg R, Durfee WK, Griffith SL, Bentley I. Optimizing the Effectiveness of a Mechanical Suture-based Anulus Fibrosus Repair Construct in an Acute Failure Laboratory Simulation. *J Spinal Disord Tech*. 2012;26(7):1. doi:10.1097/BSD.0b013e31824c8224.

17. Hart, LG. Deyo, RA. Cherkin D. Physician office visits for low back pain: frequency, clinical evaluation, and treatment patterns from a U.S. national survey. *Spine (Phila Pa 1976)*. 1995;20(1):11-19.

18. Taylor, VM. Deyo, RA. Cherkin D. Low back pain hospitalization. Recent United States trends and regional variations. *Spine (Phila Pa 1976)*. 1994;19(11):1207-1212.

19. Wipf JE, Deyo R a. Low back pain. *Med Clin North Am*. 1995;79(2):231-246.

20. Humzah, MD. Soames RW. The Anatomical Record: Human intervertebral disc: Structure and function. *Anat Rec*. 1988;220(4):337-356. doi:10.1002/ar.1092200402.

21. Smith LJ, Nerurkar NL, Choi K-S, Harfe BD, Elliott DM. Degeneration and regeneration of the intervertebral disc: lessons from development. *Dis Model Mech*. 2011;4(1):31-41. doi:10.1242/dmm.006403.

22. Roberts S, Evans H, Trivedi J, Menage J. Histology and pathology of the human intervertebral disc. *J Bone Joint Surg Am*. 2006;88 Suppl 2(suppl 2):10-14. doi:10.2106/JBJS.F.00019.

23. Urban JPG, Roberts S, Ralphs JR. The Nucleus of the Intervertebral Disc from Development to Degeneration1. *Am Zool*. 2000;40(1):53-61. doi:10.1668/0003-1569(2000)040[0053:TNOTID]2.0.CO;2.

24. EYRE, DR, Muir H. QUANTITATIVE-ANALYSIS OF TYPE-1 COLLAGEN AND TYPE-2 COLLAGEN IN HUMAN INTERVERTEBRAL DISKS AT VARIOUS AGES. *Biochim Biophys Acta*. 1977;492(1):29-42. doi:10.1016/0005-2795(77)90211-2.

25. Muir H. The Chondrocyte, Architect of Cartilage- Biomechanics, strucutre, Function, and Molecular-Biology of Cartilage Matrix Macromolecules. *Bioessays*. 1995;17(12):1039-1048. doi:10.1002/bies.950171208.

26. Antoniou, J. Steffen, T. Nelson, F. Winterbottom, N. Hollader, AP. Poole, RA. Aebi, M. Alini M. The human lumbar intervertebral disc: evidence for changes in the biosynthesis and denaturation of the extracellular matrix with growth, maturation, ageing, and degeneration. *J Clin Invest*. 1996;98(4):996-1003. doi:10.1172/JCI118884.

27. Preedy V. *Apoptosis: Modern Insights into Disease from Molecules to Man*. CRC Press; 2010.

28. Markolf KL, Morris JM. The structural components of the intervertebral disc. A study of their contributions to the ability of the disc to withstand compressive forces. *J Bone Joint Surg Am*. 1974;56(4):675-687. http://jbjs.org/content/56/4/675.abstract. Accessed June 21, 2015.

29. Jensen GM. Biomechanics of the lumbar intervertebral disk: a review. *Phys Ther*.

1980;60(6):765-773.

30. Elhussein ME. Intervertebral Disc Prolapse. 2012. http://www.slideshare.net/mohammedalhussein/intervertibral-disc-prolapse-12992189. Accessed August 8, 2015.

31. Colorado Comprehensive Spine Institute. Explaining Spinal Disorders: Lumbar Disc Herniation. 2014. http://www.coloradospineinstitute.com/subject.php?pn=cond-lumbardisc-3.

32. Freemont TJ, LeMaitre C, Watkins A, Hoyland J a. Degeneration of intervertebral discs: current understanding of cellular and molecular events, and implications for novel therapies. *Expert Rev Mol Med*. 2001;3(11):1-10. doi:10.1017/S1462399401002885.

33. Adams M a, Freeman BJ, Morrison HP, Nelson IW, Dolan P. Mechanical initiation of intervertebral disc degeneration. *Spine (Phila Pa 1976)*. 2000;25(13):1625-1636. doi:10.1097/00007632-200007010-00005.

34. Mannion a F, Adams M a, Dolan P. Sudden and unexpected loading generates high forces on the lumbar spine. *Spine (Phila Pa 1976)*. 2000;25(7):842-852. doi:10.1097/00007632-200004010-00013.

35. Horner H a, Urban JP. 2001 Volvo Award Winner in Basic Science Studies: Effect of nutrient supply on the viability of cells from the nucleus pulposus of the intervertebral disc. *Spine (Phila Pa 1976)*. 2001;26(23):2543-2549. doi:10.1097/00007632-200112010-00006.

36. Brown, MD. Malinin, TI. Davis P. A roentgenographic evaluation of frozen allografts versus autografts in anterior cervical spine fusions. *Clin Orthop Relat Res*. 1976;119:231-236.

37. Bibby SRS, Urban JPG. Effect of nutrient deprivation on the viability of intervertebral disc cells. *Eur Spine J*. 2004;13(8):695-701. doi:10.1007/s00586-003-0616-x.

38. Yang X, Li X. Nucleus pulposus tissue engineering: A brief review. *Eur Spine J*.

2009;18(11):1564-1572. doi:10.1007/s00586-009-1092-8.

39. Farhni W. Conservative treatment of lumbar disc degeneration: Our primary responsibility. *Orthop Clin North Am*. 1975;6:93-103.

40. Fitchie, JH. Farhni W. Age changes in lumbar intervertebral discs. *Can J Surg*. 1970;13:65-71.

41. Boden SD, McCowin PR, Davis DO, Dina TS, Mark AS, Wiesel S. Abnormal magnetic-resonance scans of the cervical spine in asymptomatic subjects. A prospective investigation. *J Bone Joint Surg Am*. 1990;72(8):1178-1184. http://jbjs.org/content/72/8/1178.abstract. Accessed June 29, 2015.

42. Buckwalter J. Aging and degeneration of the human intervertebral disc. *Spine (Phila Pa 1976)*. 1995;20:1307-1314.

43. Haefeli M, Elfering A, Kilian R, Min K, Boos N. Nonoperative treatment for adolescent idiopathic scoliosis: a 10- to 60-year follow-up with special reference to health-related quality of life. *Spine (Phila Pa 1976)*. 2006;31(3):355-366; discussion 367. doi:10.1097/01.brs.0000197664.02098.09.

44. Anderson DG, Tannoury C. Molecular pathogenic factors in symptomatic disc degeneration. *Spine J*. 2005;5(6 SUPPL.):260-266. doi:10.1016/j.spinee.2005.02.010.

45. Anderson DG, Albert TJ, Fraser JK, et al. Cellular therapy for disc degeneration. *Spine (Phila Pa 1976)*. 2005;30(17 Suppl):S14-S19. doi:10.1097/01.brs.0000175174.50235.ba.

46. Quint U, Wilke HJ. Grading of degenerative disk disease and functional impairment: Imaging versus patho-anatomical findings. *Eur Spine J*. 2008;17(12):1705-1713. doi:10.1007/s00586-008-0787-6.

47. Horst N. How Chiropractic Care Prevents Degeneration of the Spine. *Horst Chiropr*. 2015. http://www.horst-chiropractic.com/how-chiropractic-care-prevents-degeneration-of-the-spine/. Accessed July 22, 2015.

48. Sato K, Kikuchi S, Yonezawa T. In vivo intradiscal pressure measurement in healthy individuals and in patients with ongoing back problems. *Spine (Phila Pa 1976)*. 1999;24(23):2468-2474. doi:10.1097/00007632-199912010-00008.

49. Hestbaek L, Leboeuf-Yde C, Engberg M, Lauritzen T, Bruun NH, Manniche C. The course of low back pain in a general population. results from a 5-year prospective study. *J Manipulative Physiol Ther*. 2003;26(4):213-219. doi:10.1016/S0161-4754(03)00006-X.

50. Guterl CC, See EY, Blanquer SBG, et al. Challenges and strategies in the repair of ruptured annulus fibrosus. *Eur Cell Mater*. 2013;25:1-21. http://www.pubmedcentral.nih.gov/articlerender.fcgi?artid=3655691&tool=pmcentrez&rendertype=abstract.

51. Daffner, SD. Hymanson, HJ. Wang J. Cost and use of conservative management of lumbar disc herniation before surgical discectomy. *Spine J*. 2010;10(6):463-468.

52. Brinkmann, P. Grootenboer H. Change of disc height, radial disc bulge, and intradiscal pressure from discectomy. An in vitro investigation on human lumbar discs. *Spine (Phila Pa 1976)*. 1991;16(6):641-646. http://www.ncbi.nlm.nih.gov/pubmed/1862403.

53. Kamaric, Emri. Yeh, Oscar. Velagic, Almir. Einhorn, Jacob. Osman, Gamal. Vilandecic, Mirolad. Lambrecht G. Restoration of disc competency by increasing disc height using an annular closure device. *Spine J*. 2005;5(4):P143. doi:http://dx.doi.org/10.1016/j.spinee.2005.05.358.

54. Carragee, EJ. Spinnickie, AO. Alamin, TF. Paraqioudakis S. A Prospective Controlled Study of Limited Vs. Subtotal Posterior Discectomy: Short-Term Outcomes in Patients With Herniated Lumbar Intervertebral Discs and Large Posterior Anular Defect. *Spine (Phila Pa 1976)*. 2006;31(6):653-657. http://www.ncbi.nlm.nih.gov/pubmed/16540869.

55. Hu, RW. Jaglal, S. Axcell, T. Anderson G. A population-based study of reoperations after back surgery. *Spine (Phila Pa 1976)*. 1997;22(19):2265-2270. http://www.ncbi.nlm.nih.gov/pubmed/9346147.

56. Malter, AD. McNeney, B. Loeser, JD. Deyo R. 5-year reoperation rates after

different types of lumbar spine surgery. *Spine (Phila Pa 1976)*. 1998;23(7):814-820. http://www.ncbi.nlm.nih.gov/pubmed/9563113.

57. Atlas, SJ. Keller, RB. Chang, Y. Deyo, RA. Singer D. Surgical and nonsurgical management of sciatica secondary to a lumbar disc herniation: five-year outcomes from the Maine Lumbar Spine Study. *Spine (Phila Pa 1976)*. 2001;26(10):1179-1187. http://www.ncbi.nlm.nih.gov/pubmed/11413434.

58. Osterman, H. Sund, R. Seitsalo, S. Keskimaki I. Risk of multiple reoperations after lumbar discectomy: a population-based study. *Spine (Phila Pa 1976)*. 2003;28(6):621-627. http://www.ncbi.nlm.nih.gov/pubmed/12642772.

59. Atlas, SJ. Keller, RB. Wu, YA. Deyo, RA. Singer D. Long-Term Outcomes of Surgical and Nonsurgical Management of Sciatica to a Lumbar Herniation: 10 Year Results from the Maine Lumbar Spine Study. *Spine (Phila Pa 1976)*. 2005;30(8):927-935. http://www.ncbi.nlm.nih.gov/pubmed/15834338.

60. Ambrossi GLG et al. Recurrent lumbar disc herniation after single-level lumbar discectomy: incidence and health care cost analysis. *Neurosurgery*. 2009;65(574-578).

61. Parker SL et. al. Cost savings associated with prevention of recurrent lumbar disc herniation with a novel annular closure device: a multicenter prospective cohort study. *J Neurol Surg A Cent Eur Neruosurg*. 2013;74:285-289.

62. Choy DS. Familial incidence of intervertebral disc herniation: an hypothesis suggesting that laminectomy and discectomy may be counterproductive. *J Clin Laser Med Surg*. 2000;18(1):29-32.

63. Hegewald, AA. Ringe, J. Sittinger, M. Thome C. Regenerative treatment strategies in spinal surgery. *Front Biosci*. 2008;13:1507-1525. doi:10.2741/2777.

64. Katz JN. Lumbar disc disorders and low-back pain: socioeconomic factors and consequences. *J Bone Joint Surg Am*. 2006;88 Suppl 2(suppl 2):21-24. doi:10.2106/JBJS.E.01273.

65. Khan SN, Stirling a J. Controversial topics in surgery: degenerative disc disease:

disc replacement. Against. *Ann R Coll Surg Engl*. 2007;89(1):6-11. doi:10.1308/003588407X160792.

66. Sherman JE. Modern Spine Fusion Techniques. *Spine-health*. 2006. http://www.spine-health.com/treatment/spinal-fusion/modern-spine-fusion-techniques. Accessed June 21, 2015.

67. Orthopod. Lumbar Artifical Disc Replacement. 2015. http://www.eorthopod.com/lumbar-artificial-disc-replacement/topic/194. Accessed July 5, 2015.

68. Spivak JM. Artificial Disc Replacement or Spinal Fusion: Which is Better for You? *Spine-health*. 2006. http://www.spine-health.com/treatment/back-surgery/artificial-disc-replacement-or-spinal-fusion-which-better-you. Accessed June 21, 2015.

69. Baliga S, Treon K, Craig NJA. Low Back Pain: Current Surgical Approaches. *Asian Spine J*. 2015;9(4):645-657. doi:10.4184/asj.2015.9.4.645.

70. Kalakoti P, Missios S, Maiti T, et al. Inpatient outcomes and post-operative complications following primary versus revision lumbar spinal fusion surgeries for degenerative lumbar disc disease: A National (Nationwide) Inpatient Sample analysis 2002-2011. *World Neurosurg*. 2015:1-11. doi:10.1016/j.wneu.2015.08.020.

71. Bron JL, Helder MN, Meisel HJ, Van Royen BJ, Smit TH. Repair, regenerative and supportive therapies of the annulus fibrosus: Achievements and challenges. *Eur Spine J*. 2009;18(3):301-313. doi:10.1007/s00586-008-0856-x.

72. Walmsley R. The development and growth of the intervertebral disc. *Edinb Med J*. 1953;60(8):341-364.

73. Bruehlmann SB, Rattner JB, Matyas JR, Duncan N a. Regional variations in the cellular matrix of the annulus fibrosus of the intervertebral disc. *J Anat*. 2002;201(2):159-171. doi:10.1046/j.1469-7580.2002.00080.x.

74. Sun DDN, Leong KW. A nonlinear hyperelastic mixture theory model for

anisotropy, transport, and swelling of annulus fibrosus. *Ann Biomed Eng*. 2004;32(1):92-102. doi:10.1023/B:ABME.0000007794.87408.1e.

75. Weinstein, Stuart. Buckwalter J. *Turek's Orthopaedics: Principles and Their Application*. Vol 6th Editio. Lippincott Williams & Wilkins; 2005.

76. Horner H a, Horner H a, Roberts S, et al. Cells from different regions of the intervertebral disc: effect of culture system on matrix expression and cell phenotype. *Spine (Phila Pa 1976)*. 2002;27(10):1018-1028. http://www.ncbi.nlm.nih.gov/pubmed/12004167.

77. Adams, P. Eyre, DR. Muir H. Biochemical aspects of development and ageing of human lumbar intervertebral discs. *Rheumatol Rehabil*. 1977;16:22-29.

78. Hayes a. J, Benjamin M, Ralphs JR. Extracellular matrix in development of the intervertebral disc. *Matrix Biol*. 2001;20(2):107-121. doi:10.1016/S0945-053X(01)00125-1.

79. Hayes AJ, Smith SM, Gibson M a., Melrose J. Comparative Immunolocalization of the Elastin Fiber–Associated Proteins Fibrillin-1, LTBP-2, and MAGP-1 With Components of the Collagenous and Proteoglycan Matrix of the Fetal Human Intervertebral Disc. *Spine (Phila Pa 1976)*. 2011;36(21):E1365-E1372. doi:10.1097/BRS.0b013e31821fd23e.

80. Eyre DR, Muir H. Types I and II collagens in intervertebral disc. Interchanging radial distributions in annulus fibrosus. *Biochem J*. 1976;157(1):267-270.

81. Rufai, A. Benjamin, M. Ralphs J. The development of fibrocartilage in the rat intervertebral disc. *Anat Embryol*. 1995;192:53-62.

82. Hayes, AJ. Issacs, MD. Hughes, C. Caterson, B. Ralphs J. Collagen fibrillogenesis in the development of the annulus fibrosus of the intervertebral disc. *Eur Cell Mater*. 2011;22:226-241.

83. Singh K, Masuda K, Thonar EJ-M a, An HS, Cs-Szabo G. Age-related changes in the extracellular matrix of nucleus pulposus and anulus fibrosus of human intervertebral disc. *Spine (Phila Pa 1976)*. 2009;34(1):10-16.

doi:10.1097/BRS.0b013e31818e5ddd.

84. Pattappa G, Li Z, Peroglio M, Wismer N, Alini M, Grad S. Diversity of intervertebral disc cells: Phenotype and function. *J Anat*. 2012;221(6):480-496. doi:10.1111/j.1469-7580.2012.01521.x.

85. Jin L, Shimmer AL, Li X. The challenge and advancement of annulus fibrosus tissue engineering. *Eur Spine J*. 2013;22(5):1090-1100. doi:10.1007/s00586-013-2663-2.

86. Best, BA. Guilak, F. Setton L. Compressive mechanical properties of the human anulus fibrosus and their relationship to biochemical composition. *Spine (Phila Pa 1976)*. 1994;19(2):212-221.

87. Setton LA, Chen J. Mechanobiology of the intervertebral disc and relevance to disc degeneration. *J Bone Joint Surg Am*. 2006;88 Suppl 2(suppl 2):52-57. doi:10.2106/JBJS.F.00001.

88. Loy, Fung. Taoist, Kok. Chi T. Notes on Anatomy and Physiology: The Intervertebral Discs. *From Tiger's Mouth*. 2015. https://ittcs.wordpress.com/2010/06/01/anatomy-and-physiology-the-intervertebral-discs/. Accessed July 15, 2015.

89. Yu J, Tirlapur U, Fairbank J, et al. Microfibrils, elastin fibres and collagen fibres in the human intervertebral disc and bovine tail disc. *J Anat*. 2007;210(4):460-471. doi:10.1111/j.1469-7580.2007.00707.x.

90. Yu J, Fairbank JCT, Roberts S, Urban JPG. The elastic fiber network of the anulus fibrosus of the normal and scoliotic human intervertebral disc. *Spine (Phila Pa 1976)*. 2005;30(16):1815-1820. doi:10.1097/01.brs.0000173899.97415.5b.

91. Pezowicz C a., Robertson P a., Broom ND. The structural basis of interlamellar cohesion in the intervertebral disc wall. *J Anat*. 2006;208(3):317-330. doi:10.1111/j.1469-7580.2006.00536.x.

92. Smith LJ, Fazzalari NL. Regional variations in the density and arrangement of elastic fibres in the anulus fibrosus of the human lumbar disc. *J Anat*.

2006;209(3):359-367. doi:10.1111/j.1469-7580.2006.00610.x.

93. McNally, DS. Adams M. Internal intervertebral disc mechanics as revealed by stress profilometry. *Spine (Phila Pa 1976)*. 1992;17(1):66-73. doi:10.1097/00007632-199201000-00011.

94. Stokes I. Surface strain on human intervertebral discs. *J Orthop Res*. 1987;5(3):348-355. doi:10.1002/jor.1100050306.

95. Melrose, J. Smith, SM. Appleyard, RC. Little C. Aggrecan, versican and type VI collagen are components of annular Eur Spine J (2009) 18:301–313 311 123 translamellar crossbridges in the intervertebral disc. *Eur Spine J*. 2008;17(2):314-324. doi:10.1007/s00586-007-0538-0.

96. Marchand, F. Ahmed A. Investigation of the laminate structure of lumbar disc anulus fibrosus. *Spine (Phila Pa 1976)*. 1990;15(5):402-410. doi:10.1097/00007632-199005000-00011.

97. Smith LJ, Byers S, Costi JJ, Fazzalari NL. Elastic fibers enhance the mechanical integrity of the human lumbar anulus fibrosus in the radial direction. *Ann Biomed Eng*. 2008;36(2):214-223. doi:10.1007/s10439-007-9421-8.

98. Edwards WT, Ordway NR, Zheng Y, McCullen G, Han Z, Yuan H a. Peak stresses observed in the posterior lateral anulus. *Spine (Phila Pa 1976)*. 2001;26(16):1753-1759. doi:10.1097/00007632-200108150-00005.

99. Osti OL, Vernon-Roberts B, Moore R, Fraser RD. Annular tears and disc degeneration in the lumbar spine. A post-mortem study of 135 discs. *J Bone Joint Surg Br*. 1992;74(5):678-682.

100. Zhong W, Driscoll SJ, Wu M, et al. In Vivo Morphological Features of Human Lumbar Discs. *Medicine (Baltimore)*. 2014;93(28):e333. doi:10.1097/MD.0000000000000333.

101. Green, T P. Adams, M A. Dolan P. Tensile Properties of the Annulus Fibrosus II. Ultimate Tensile Strength and fatigue life. *Eur Spine J*. 1993;2:209-214.

102. O'Connell GD, Sen S, Elliott DM. Human annulus fibrosus material properties from biaxial testing and constitutive modeling are altered with degeneration. *Biomech Model Mechanobiol*. 2012;11(3-4):493-503. doi:10.1007/s10237-011-0328-9.

103. Ahlgren BD, Lui W, Herkowitz HN, Panjabi MM, Guiboux JP. Effect of anular repair on the healing strength of the intervertebral disc: a sheep model. *Spine (Phila Pa 1976)*. 2000;25(17):2165-2170. doi:10.1097/00007632-200009010-00004.

104. Ethier, DB. Cain, JE. Yaszemski M. The influence of anulotomy selection on disc competence. A radiographic, biomechanical, and histologic analysis. *Spine (Phila Pa 1976)*. 1994;19(18):2071-2076. doi:10.1097/00007632-199409150-00012.

105. Ganey, T. Libera, J. Moos V. Disc chondrocyte transplantation in a canine model: a treatment for degenerated or damaged intervertebral disc. *Spine (Phila Pa 1976)*. 2003;28(23):2609-2620. doi:10.1097/01.BRS.0000097891.63063.78.

106. Hampton, D. Laros, G. McCarron, R. Franks D. Healing potential of the anulus fibrosus. *Spine (Phila Pa 1976)*. 1989;14(4):398-401. doi:10.1097/00007632-198904000-00009.

107. Key JA, Ford LT. EXPERIMENTAL INTERVERTEBRAL-DISC LESIONS. *J Bone Jt Surg*. 1948;30(3):621-630. http://jbjs.org/content/30/3/621.abstract. Accessed June 25, 2015.

108. Melrose J, Ghosh P, Taylor TKF, Vernon-Roberts B, Latham J, Moore R. Elevated synthesis of biglycan and decorin in an ovine annular lesion model of experimental disc degeneration. *Eur Spine J*. 1997;6(6):376-384. doi:10.1007/BF01834063.

109. Moore, RJ. Osti, OL. Vernon-Robers, B. Fraser R. Changes in endplate vascularity after an outer anulus tear in the sheep. *Spine (Phila Pa 1976)*. 1992;17(8):874-878. doi:10.1097/00007632-19920 8000-00003.

110. Osti, OL. Vernon-Roberts, B. Fraser R. 1990 Volvo Award in experimental studies. Anulus tears and intervertebral disc degeneration. An experimental study using an animal model. *Spine (Phila Pa 1976)*. 1990;15(8):762-767. doi:10.1097/00007632-19900 8010-00005.

111. Rousseau M-A a, Ulrich J a, Bass EC, Rodriguez AG, Liu JJ, Lotz JC. Stab incision for inducing intervertebral disc degeneration in the rat. *Spine (Phila Pa 1976)*. 2007;32(1):17-24. doi:10.1097/01.brs.0000251013.07656.45.

112. Smith JW, Walmsley R. Experimental incision of the intervertebral disc. *J Bone Joint Surg Br*. 1951;33-B(4):612-625.

113. Korecki CL, Costi JJ, Iatridis JC. Needle puncture injury affects intervertebral disc mechanics and biology in an organ culture model. *Spine (Phila Pa 1976)*. 2008;33(3):235-241. doi:10.1097/BRS.0b013e3181624504.

114. Guerin HL, Elliott DM. Quantifying the contributions of structure to annulus fibrosus mechanical function using a nonlinear, anisotropic, hyperelastic model. *J Orthop Res*. 2007;25(4):508-516.

115. Iatridis JC, Ap Gwynn I. Mechanisms for mechanical damage in the intervertebral disc annulus fibrosus. *J Biomech*. 2004;37(8):1165-1175. doi:10.1016/j.jbiomech.2003.12.026.

116. Leung VYL, Chan D, Cheung KMC. Regeneration of intervertebral disc by mesenchymal stem cells: Potentials, limitations, and future direction. *Eur Spine J*. 2006;15(SUPPL. 3). doi:10.1007/s00586-006-0183-z.

117. Shao X, Hunter CJ. Developing an alginate/chitosan hybrid fiber scaffold for annulus fibrosus cells. *J Biomed Mater Res - Part A*. 2007. doi:10.1002/jbm.a.31030.

118. Chang G, Kim HJ, Kaplan D, Vunjak-Novakovic G, Kandel R a. Porous silk scaffolds can be used for tissue engineering annulus fibrosus. *Eur Spine J*. 2007;16(11):1848-1857. doi:10.1007/s00586-007-0364-4.

119. Mizuno H, Roy AK, Vacanti C a, Kojima K, Ueda M, Bonassar LJ. Tissue-engineered composites of anulus fibrosus and nucleus pulposus for intervertebral disc replacement. *Spine (Phila Pa 1976)*. 2004;29(12):1290-1297; discussion 1297-1298. doi:10.1097/01.BRS.0000128264.46510.27.

120. Nerurkar NL, Elliott DM, Mauck RL. Mechanics of oriented electrospun nanofibrous scaffolds for annulus fibrosus tissue engineering. *J Orthop Res*. 2007. doi:10.1002/jor.20384.

121. Wan Y, Feng G, Shen FH, Balian G, Laurencin CT, Li X. Novel biodegradable poly(1,8-octanediol malate) for annulus fibrosus regeneration. *Macromol Biosci*. 2007;7(11):1217-1224. doi:10.1002/mabi.200700053.

122. Helen W, Gough JE. Cell viability, proliferation and extracellular matrix production of human annulus fibrosus cells cultured within PDLLA/Bioglass® composite foam scaffolds in vitro. *Acta Biomater*. 2008;4(2):230-243. doi:10.1016/j.actbio.2007.09.010.

123. Wan Y, Feng G, Shen FH, Laurencin CT, Li X. Biphasic scaffold for annulus fibrosus tissue regeneration. *Biomaterials*. 2008;29(6):643-652. doi:10.1016/j.biomaterials.2007.10.031.

124. Sato M, Asazuma T, Ishihara M, et al. An atelocollagen honeycomb-shaped scaffold with a membrane seal (ACHMS-scaffold) for the culture of annulus fibrosus cells from an intervertebral disc. *J Biomed Mater Res A*. 2003;64(2):248-256. doi:10.1002/jbm.a.10287.

125. Roughley PJ. Biology of intervertebral disc aging and degeneration: involvement of the extracellular matrix. *Spine (Phila Pa 1976)*. 2004;29(23):2691-2699. doi:10.1097/01.brs.0000146101.53784.b1.

126. Risbud M V, Guttapalli A, Tsai T-T, et al. Evidence for skeletal progenitor cells in the degenerate human intervertebral disc. *Spine (Phila Pa 1976)*. 2007;32(23):2537-2544. doi:10.1097/BRS.0b013e318158dea6.

127. Vergroesen P-P a., Bochyńska AI, Emanuel KS, et al. A Biodegradable Glue For Annulus Closure. *Spine (Phila Pa 1976)*. 2015;40(9):1. doi:10.1097/BRS.0000000000000792.

128. Guillaume O, Naqvi SM, Lennon K, Buckley CT. Enhancing cell migration in shape-memory alginate-collagen composite scaffolds: In vitro and ex vivo assessment for intervertebral disc repair. *J Biomater Appl*. 2014;29(9):1230-1246. doi:10.1177/0885328214557905.

129. Emans PJ, Pieper J, Hulsbosch MM, et al. Differential cell viability of chondrocytes and progenitor cells in tissue-engineered constructs following implantation into osteochondral defects. *Tissue Eng*. 2006;12(6):1699-1709. doi:10.1089/ten.2006.12.ft-148.

130. Pirvu T, Blanquer SBG, Benneker LM, et al. A combined biomaterial and cellular approach for annulus fibrosus rupture repair. *Biomaterials*. 2015;42:11-19. doi:10.1016/j.biomaterials.2014.11.049.

131. Guillaume O, Daly A, Lennon K, Gansau J, Buckley SF, Buckley CT. Shape-memory porous alginate scaffolds for regeneration of the annulus fibrosus: Effect of TGF-β3 supplementation and oxygen culture conditions. *Acta Biomater*. 2014;10(5):1985-1995. doi:10.1016/j.actbio.2013.12.037.

132. Driscoll TP, Nakasone RH, Szczesny SE, Elliott DM, Mauck RL. Biaxial mechanics and inter-lamellar shearing of stem-cell seeded electrospun angle-ply laminates for annulus fibrosus tissue engineering. *J Orthop Res*. 2013;31(6):864-870. doi:10.1002/jor.22312.

133. Sharifi S, van Kooten TG, Kranenburg HJC, et al. An annulus fibrosus closure device based on a biodegradable shape-memory polymer network. *Biomaterials*. 2013;34(33):8105-8113. doi:10.1016/j.biomaterials.2013.07.061.

134. Cho H, Park SH, Park K, et al. Construction of a tissue-engineered annulus fibrosus. *Artif Organs*. 2013;37(7). doi:10.1111/aor.12066.

135. Vadalà G, Mozetic P, Rainer A, et al. Bioactive electrospun scaffold for annulus fibrosus repair and regeneration. *Eur Spine J*. 2012;21(SUPPL. 1):20-27. doi:10.1007/s00586-012-2235-x.

136. Chan SCW, Gantenbein-Ritter B. Intervertebral disc regeneration or repair with biomaterials and stem cell therapy - Feasible or fiction? *Swiss Med Wkly*. 2012;142(MAY):1-12. doi:10.4414/smw.2012.13598.

137. See, Eugene Yong-Shun. Toh, Siew Lok. Goh JCH. Simulated intervertebral disc-like assembly using bone marrow-derived mesenchymal stem cell sheets and silk

scaffolds for annulus fibrosus regeneration. *J Tissue Eng Regen Med*. 2012;6:528-535. doi:10.1002/term.

138. Chang G, Kim HJ, Vunjak-Novakovic G, Kaplan DL, Kandel R. Enhancing annulus fibrosus tissue formation in porous silk scaffolds. *J Biomed Mater Res - Part A*. 2010;92(1):43-51. doi:10.1002/jbm.a.32326.

139. Wilda H, Gough JE. In vitro studies of annulus fibrosus disc cell attachment, differentiation and matrix production on PDLLA/45S5 Bioglass?? composite films. *Biomaterials*. 2006;27(30):5220-5229. doi:10.1016/j.biomaterials.2006.06.008.

140. Sato M, Asazuma T, Ishihara M, et al. An experimental study of the regeneration of the intervertebral disc with an allograft of cultured annulus fibrosus cells using a tissue-engineering method. *Spine (Phila Pa 1976)*. 2003;28(6):548-553. doi:10.1097/01.BRS.0000049909.09102.60.

141. Wilke HJ, Heuer F, Neidlinger-Wilke C, Claes L. Is a collagen scaffold for a tissue engineered nucleus replacement capable of restoring disc height and stability in an animal model? *Eur Spine J*. 2006;15(SUPPL. 3). doi:10.1007/s00586-006-0177-x.

142. Andersson GBJ, An HS, Oegema TR, Setton LA. Directions for future research. *J Bone Joint Surg Am*. 2006;88 Suppl 2(suppl 2):110-114. doi:10.2106/JBJS.F.00030.

143. Tortora, Gerard J. Nielsen MT. *Principles of Human Anatomy (11th Ed.).* Vol (Sons JW&, ed.).; 2009.

144. Tedder ME, Liao J, Weed B, et al. Stabilized collagen scaffolds for heart valve tissue engineering. *Tissue Eng Part A*. 2009;15(6):1257-1268. doi:10.1089/ten.tea.2008.0263.

145. Burden D. Guide to the homogenization of biological samples. *Random Prim*. 2008;(7):1-14. http://opsdiagnostics.com/notes/ranpri/Homogenization Guide ver.1.pdf.

146. En ME, Machine P, Topic D. Contact Stresses and Deformations Curved Surfaces

in Contact – Examples. :1-10.

147. McGuire R. THE DEVELOPMENT OF A BIOMIMETIC PATCH FOR ANNULUS FIBROSUS REPAIR. 2015.

148. Yue, James J. Bertagnoli, Rudolf. McAfee, Paul C. An HS. *Motion Preservation Surgery of the Spine. Advanced Thechniques and Controversies.* Vol (Murphy, Kimberly. Brigido A, ed.). Philadephia: Elsevier Inc.; 2008.

149. Wilke H-J, Widmann L, Graf N, Heuer F. Can Herniation Be Prevented? Establishment of a Herniation Model and Experiments with an Annulus Reconstruction Implant. *Spine J*. 2011;11(10):S148-S149. doi:10.1016/j.spinee.2011.08.358.

150. Olmarker K. Neovascularization and neoinnervation of subcutaneously placed nucleus pulposus and the inhibitory effects of certain drugs. *Spine (Phila Pa 1976)*. 2005;30(13):1501-1504. doi:00007632-200507010-00007 [pii].

151. Nygaard OP, Mellgren SI, Osterud B. The inflammatory properties of contained and noncontained lumbar disc herniation. *Spine (Phila Pa 1976)*. 1997;22(21):2484-2488. doi:10.1097/00007632-199711010-00004.

152. Coppes MH, Marani E, Thomeer RT, Groen GJ. Innervation of "painful" lumbar discs. *Spine (Phila Pa 1976)*. 1997;22(20):2342-2349; discussion 2349-2350. http://www.ncbi.nlm.nih.gov/pubmed/9355214.

153. Iatridis, James C. Nicoll, Steven B. Michalek, Arthur J. Walter, Benjamin A. Gupta MS. Role of biomechanics on intervertebral disc degeneration and regenerative therapies: What needs repairing in the disc and what are promising biomaterials for its repair? *Spine J*. 2013;13(3):243-262. doi:10.1016/j.spinee.2012.12.002.

154. Zhou SH, McCarthy ID, McGregor a H, Coombs RR, Hughes SP. Geometrical dimensions of the lower lumbar vertebrae--analysis of data from digitised CT images. *Eur Spine J*. 2000;9(3):242-248. doi:10.1007/s005860000140.

155. Hasan M, Alam a KMM. Application of electrospinning techniques for the

production of tissue engineering scaffolds : A Review. 2014;10(15):265-278.

156. Mills C. M1 and M2 Macrophages: Oracles of Health and Disease. *Crit Rev Immunol*. 2012;32(6):463-488.

157. Brown BN, Badylak SF. Extracellular matrix as an inductive scaffold for functional tissue reconstruction. *Transl Res*. 2014;163(4):268-285. doi:10.1016/j.trsl.2013.11.003.

158. Xu H, Xu B, Yang Q, et al. Comparison of decellularization protocols for preparing a decellularized porcine annulus fibrosus scaffold. *PLoS One*. 2014;9(1):1-13. doi:10.1371/journal.pone.0086723.

159. Keane TJ, Londono R, Turner NJ, Badylak SF. Consequences of ineffective decellularization of biologic scaffolds on the host response. *Biomaterials*. 2012;33(6):1771-1781. doi:10.1016/j.biomaterials.2011.10.054.

160. Mirnajafi A, Raymer J, Scott MJ, Sacks MS. The effects of collagen fiber orientation on the flexural properties of pericardial heterograft biomaterials. *Biomaterials*. 2005;26:795-804. doi:10.1016/j.biomaterials.2004.03.004.

161. Holzapfel, Gerhard A. Ogden RW. *Mechanics of Biological Tissue*. Vol (Holzapfel, Gerhard A. Ogden RW, ed.).; 2006.

162. Qing L et al. *Tissue Regeneration Where Nano-Strucutre Meets Biology*. Vol (Liu, Qing. Wang H, ed.). WSPC; 2014.

163. Campbell FC. Chapter 1: Introduction to Composite Materials. *Manuf Process Adv Compos*. 2010:30.

164. White, Augustus A. Panjabi MM. *Clinical Biomechanics of the Spine*. Vol 2nd Editio. Philadelphia: Lippincott Williams & Wilkins; 1990.

165. Ambard D, Cherblanc F. Mechanical behavior of annulus fibrosus: A microstructural model of fibers reorientation. *Ann Biomed Eng*. 2009;37(11):2256-2265. doi:10.1007/s10439-009-9761-7.

166. Adams MA. Mechanical Properties of Aging Soft Tissues. 2015. doi:10.1007/978-3-319-03970-1.

167. Iencean SM. Lumbar intervertebral disc herniation following experimental intradiscal pressure increase. *Acta Neurochir (Wien)*. 2000;142(6):669-676. doi:10.1007/s007010070111.

168. Galante JO. Tensile properties of the human lumbar annulus fibrosus. *Acta Orthop Scand*. 1967;(100):Suppl 100:1-91.

169. Wilke HJ, Neef P, Caimi M, Hoogland T, Claes LE. New in vivo measurements of pressures in the intervertebral disc in daily life. *Spine (Phila Pa 1976)*. 1999;24(8):755-762. doi:10.1097/00007632-199904150-00005.

170. Nightingale RW, McElhaney JH, Richardson WJ, Myers BS. Dynamic responses of the head and cervical spine to axial impact loading. *J Biomech*. 1996;29(3):307-318. doi:10.1016/0021-9290(95)00056-9.

171. Duma S et al. Biomechanical response of the lumbar spine in dynamic compression. *Biomed Sci Instrum*. 2006;42:476.

172. Elias, Paul Z. Nuckley DJ. Effect of Loading Rate on the Compressive Mechanics of the Immature Baboon Cervical Spine. *J Biomech Eng*. 2005;128(1):18-23. doi:10.1115/1.2133767.

173. Yoganandan N, Kumaresan S, Pintar F a. Biomechanics of the cervical spine. Part 2. Cervical spine soft tissue responses and biomechanical modeling. *Clin Biomech*. 2001;16(1):1-27. doi:10.1016/S0268-0033(00)00074-7.

174. Cassidy J. The response of the hierarchical structure of the intervertebral disc to uniaxial compression. *J Mater Sci Mater Med*. 1990;1(2):69-80.

175. Howard D, Buttery LD, Shakesheff KM, Roberts SJ. Tissue engineering: strategies, stem cells and scaffolds. *J Anat*. 2008;213(1):66-72. doi:10.1111/j.1469-7580.2008.00878.x.

176. Cox, Thomas. Erler J. Remodeling and homeostasis of the extracellular matrix:

implications for fibrotic diseases and cancer. *Dis Model Mech*. 2011;4(2):165-178. doi:10.1242/dmm.004077.